Vol. 2 August, 1959 No. 6

MINERALOGICAL JOURNAL

CONTENTS

Mineralogical Study on the Stone in Glass.....T. Fukui....355

Variation of Unit Cell Parameters in Wolframite Series ....
.....A. Sasaki....375

Ikunolite, A New Bismuth Mineral from the Ikuno Mine, Japan.....A. Kato....397

The Minerals of the Noda-Tamagawa Mine, Iwaté Prefecture, Japan. I. Notes on Geology and Parageneses of Minerals
..... T. Watanabe....408

Short Communications

Melilite Crystal in the Cavity of Blast-Furnace Slag.....
.....H. Minato....422

Abstract of the Kobutsugaku Zasshi, Journal of the Mineralogical Society of Japan, Vol. 4, Nos. 1-2.....427

Index to Volume 2 431

Title-page and Contents

The Mineralogical Society of Japan
Chigaku Center, Niban-cho,
Chiyoda-ku, Tokyo

MINERALOGICAL JOURNAL

published by

The Mineralogical Society of Japan

EDITORIAL BOARD

Zyunpéi HARADA, *Hokkaido University;* Teiichi ITO, *University of Kyoto;* (Chief) Nobuo KATAYAMA, *University of Tokyo;* Keiichi OMORI, *Tohoku University;* Ryôiti KIRIYAMA, *University of Osaka;* Seitaro TSUBOI, *University of Tokyo;* Takeo WATANABE, *University of Tokyo;* Toyofumi YOSHIMURA, *Kyushu University.*

Instructions to Contributors

Manuscripts of articles should be submitted to the executive editor, Nobuo Katayama, at the College of General Education, University of Tokyo, Komaba, Meguro-ku, Tokyo. The manuscript should be type-written with double space lines, and not exceed 20 sheets of normal type-writing paper. References of literature should be in accordance with the forms used in the pages of this journal.

Plates and figures should be capable of reduction to not more than 10 by 15 centimeters. Line drawings should be in black India ink on white drawing board, tracing paper, or coordinate paper printed in blue. Photographs should be positive glossy prints.

Two referees chosen by the Editorial Board read the manuscript of article submitted before it is accepted for publication.

Thirty reprints without cover will be furnished to the author free of cost and without previous notice from him. Additional reprints will be furnished at cost when ordered.

The price of the journal to subscribers in Japan is 250 yen for a single copy (including postage), and to subscribers in other countries $ 1.00 (including postage) for a single copy, or $ 5.00 (including postage) per volume of 6 numbers.

Printed in Japan

Mineralogical Journal, Vol. 2, No. 6, pp. 355-374, Aug., 1959

MINERALOGICAL STUDY ON THE STONE IN GLASS

Tadaoki Fukui

Research Laboratory, Asahi Glass Co.

Abstract

Morphological, optical and X-ray properties of several stones in glass were described and considerations were made of the geneses of these stones.

It has been found that the difference in the variety of the stones arises from the difference in compositions of molten glass itself and/or of refracory bricks. In addition, foreign materials which have been captured in the molten glass also affect the character of stones.

The writer found new occurrences of aegirine, celsian, hercynite and spinel in stones.

Introduction

The stone in glass is defined as the contamination substance in glass and glassware, and usually it consists of or contains crystalline materials.

The specimens described in the present paper are the stones which have been found in the glasswares manufactured mostly by means of tank furnaces. The outline of the manufacturing process, is as follows: Glass tank furnace usually consists of melting, refining and working areas. Batch materials, containing quartz sand, sodium carbonate and sulfate, dolomite, feldspar and others, are fed into the melting area, in which they melt at 1400°~1500°C.. On the course from the melting area to the working area through the refining one, the molten glass is refined and cooled down to 950°~1050°C., until it is continuously pulled out and molded as finished wares. The tank furnace is adequately constructed of various kinds of refractory bricks capable of withstanding the chemical and ther-

Table 1. Chemical compositions of glasses.

	Soda-lime-silica glass		Alkali-less glass	BaO-bearing glass (Braun tube glass)
	(plate glass)	(tube glass)	(fiber glass)	
SiO_2	71.87%	73.31%	55.40%	67.16%
Al_2O_3	1.71	1.14	17.39	6.29
Fe_2O_3	0.09	0.13	0.18	0.08
TiO_2	0.23	tr.	0.70	——
CaO	7.93	4.73	12.28	——
MgO	3.99	3.41	5.98	——
Na_2O	13.93	16.49	0.15	8.82
K_2O	——	0.08	0.23	5.02
SO_3	0.25	——	——	0.15
BaO	——	0.34	6.13	11.38

(Anal. The Research Laboratory, Asahi Glass Co.)

Table 2. Chemical compositions and constituent minerals of refractories.

	Fireclay refractory		High-aluminous refractory		Electrofused zirconia refractory
	low-aluminous	high-aluminous	molded refractory	electro-fused refractory	
SiO_2	57.65%	48.60%	23.87%	20.01%	12.27%
Al_2O_3	36.00	46.85	73.00	76.63	51.09
Fe_2O_3	2.46	1.78	1.82	1.06	0.41
TiO_2	1.23	1.80	1.12	1.80	0.81
CaO	0.29	0.19	0.38	0.30	0.32
MgO	0.29	0.07	0.21	0.20	0.14
R_2O	——	——	——	——	1.04
ZrO_2	——	——	——	——	34.63
constituent minerals	mullite quartz glassy matrix	mullite glassy matrix	mullite corundum glassy matrix	mullite corundum glassy matrix	baddeleyite corundum glassy matrix

(Anal. The Research Laboratory, Asahi Glass Co.)

mal conditions to which they are exposed. The chemical compositions of the glasses under consideration and those of the refractories relevant to the present investigation are given in Tables 1 and 2 respectively.

The stone in glass may be divided into three types according to its origin: (1) The relic of batch materials or impurities in them. Mineral phases usually found in the stone of this type are quartz, sodium sulfate, feldspar, dolomite, various metals, hematite, magnetite, chromite, clay minerals and so on. (2) Fragments of refractories or of reaction products between refractories and glasses. Besides the constituent minerals of refractories given in Table 2, crystals of nepheline, carnegieite, corundum, β-alumina and tridymite are common in this type of stones. (3) Products of devitrification of the glass; wollastonite, devitrite, diopside, cristobalite and tridymite.

In the course of this study the writer has discovered several stones with distinct constituent minerals which were not fully described by previous investigators[3) 5) 6) 7) 8) 14) 15)]. The minerals are diopside and aegirine both produced by devitrification, and celsian, hercynite and spinel which are the reaction products between refractories and glasses. The minerals of the latter group may be regarded as a modification, under a special condition, of nepheline or corundum, i. e. the normal reaction products, so investigations into these two stone minerals were also carried out.

Properties of pyroxene stones

(1) *Diopside stone* The diopside stone found in the ordinary soda-lime-silica glass consists of a large number of prismatic or acicular crystals 0.1~0.5 mm. in length, their longitudinal direction being parallel to c-axis. The faces (100), (010), $(\bar{1}11)$ and $(\bar{1}21)$ are observed under the microscope. Optical properties are: $Z \wedge c = 41° \pm 1°$, $Y = b$; $(+)2V = 61° \pm 2°$; $\alpha = 1.672 \pm 0.001$, $\beta \fallingdotseq 1.685$ (calc.), $\gamma = 1.702 \pm 0.001$, $\gamma - \alpha \fallingdotseq 0.030$.

A remarkable occurrence of diopside stone was found in an alkali-

less glass of which the chemical composition is given in Table 1. The stone contains four diopside crystals which form well-grown envelope-like shapes with almost the same size of about $2 \times 5 \times 12$ mm.. They partly penetrate each other to form a chain as shown in Fig. 1 (Plate I), but the mode of penetration does not suggest any regular twinning rule. Many minute crystallites of diopside and some fragments of iron are found scattering in the surrounding glass of the stone.

All the crystals are of the same habit with faces (130) and ($\bar{1}51$). The interfacial angles were roughly measured by means of universal stage under the microscope: $130 \wedge \bar{1}30 \fallingdotseq 35°$ (35°12′½ according to E.S. Dana's "A System of Mineralogy") and $\bar{1}51 \wedge \bar{1}\bar{5}1 \fallingdotseq 143°$ (calc.=141°24′). As shown in Fig. 2 (Plate I), however, skeletal structure with interstitial glass was observed under the microscope, and it was also revealed that the faces (130) and ($\bar{1}51$) were composed of repetitions of (110) and ($\bar{1}31$) respectively.

Optical properties are: $Z \wedge c = 38° \pm 1°$, $Y = b$; $(+)2V = 60° \pm 2°$; $\alpha = 1.671 \pm 0.002$, $\beta \fallingdotseq 1.683$ (calc.), $\gamma = 1.701 \pm 0.002$; $\gamma - \alpha \fallingdotseq 0.030$. According to the Winchell's variation diagram[16] of optical constants versus chemical composition of the diopside-hedenbergite system, those optical properties correspond to the 90% diopside phase in this binary system.

X-ray powder diffraction data are given in Table 3. The specimen for X-ray examination was ground and then treated with bromoform, but it was difficult to separate the diopside crystals completely from the surrounding glass, so the intensity of the powder pattern obtained from this specimen was not so strong. When, however, the X-ray data of this stone are compared with those of the artificial diopsides reported by H.S. Yoder[18] and C.B. Clark[2], the main diffraction lines of diopside are sufficiently recognized. Among these lines, the strongest diffraction line of magnetite (Fe_3O_4), which is enclosed in the surrounding glass of the diopside crystals, is also recognized.

Table 3. X-ray powder data for the diopside stone.

Diopside stone		Artificial diopside			
		H. S. Yoder, Jr.[18]		C. B. Clark[2]	
I	d(Å)	I	d(Å)	I	d(Å)
75	3.351	10	3.33	vvw	3.34
85	3.227	40	3.22	vw	3.22
75	3.018 3.003	100	2.98	S	2.99
50	2.940	30	2.94	vvw	2.95
100	2.903 2.894	40	2.88	w	2.89
75	2.561	30	2.56	vvw	2.56
60	2.538*				
100	2.522 2.508	80	2.52	S	2.52
50	2.380 2.368	5	2.39		
65	2.296	20	2.29	vvw	2.30
55	2.206 2.196	10 10	2.21 2.19	vvw vvw	2.21 2.19
65	2.150	20	2.146	vvw	2.15
50	2.127	50	2.121	vw	2.13
30	2.106	10	2.101	vvw	2.10
75	2.040	30	2.034	vw	2.04
30	2.006	20	2.008	vvw	2.01
		10	1.954	vvw	1.967
55	1.860	5	1.853		
20	1.826	10	1.828	vvw	1.830
30	1.796	5	1.806		
55	1.752 1.749	20	1.750	vw	1.745
		10	1.670	vvw	1.664
		10	1.656	vvw	1.659
30	1.621	30	1.620	M	1.617
30	1.558	5	1.559	vvw	1.556
		10	1.548	vvw	1.542
		10	1.524	vvw	1.522
20	1.492			vvw	1.497
20	1.484			vvw	1.485

* The strongest diffraction line of Fe_3O_4.

(2) *Aegirine stone* Aegirine stones found by the author are divided into two groups: one is diopside-rich, the other acmite-rich. They are not so rare, but no previous paper has described their occurrence.

The diopside-rich aegirine is seldom found in soda-lime-silica glass as aggregates of prismatic grass-green crystals surrounding small fragments of iron oxide. Since some of the crystals, with lengths up to about 0.5 mm., are observed to have edges [100], [$\bar{1}$01], [010], [011] and [021] under the microscope (Fig. 3, Plate I), it is supposed that they consist of faces (100), (010), ($\bar{1}$11) and ($\bar{1}$21). Optical properties are: $Z \wedge c = 48° \pm 2°$, $Y = b$; $(+)2V = 70° \pm 3°$; $\alpha = 1.70 \pm 0.005$, $\beta \fallingdotseq 1.71$ (calc.), $\gamma = 1.73 \pm 0.005$, $\gamma - \alpha \fallingdotseq 0.03$; pleochroism, X=grass green, Y=yellowish green, Z=yellowish orange. These properties correspond to the phase of 75% diopside in the optical constants versus chemical composition diagram for the diopside-acmite system established by I. A. Ostrovsky[11] and K. Yagi[17].

The acmite-rich aegirine stones rather frequently occur surrounding hematite grains due to iron rust which dropped into the molten soda-lime-silica glass. They consist of prismatic yellowish brown crystals (Fig. 4, Plate I) with lengths up to 0.1 mm. (rarely up to 0.5 mm. max.). The glass adjacent to them is of yellow colour with refractive indices up to $n = 1.60$, while that of the mother glass is $n = 1.518$. Observed main crystal faces are (110), ($\bar{1}$11) and ($\bar{1}$21), with sporadic minute faces (100), (010) and (001). Cleavage parallel to (110) is distinct. Zonal growths are observed on some of the crystals. Optical properties for one of the crystals are: $X \wedge c = -5° \pm 1°$, $Y = b$; $(-)2V = 63° \pm 2°$; $\alpha = 1.756 \pm 0.001$, β and γ=n. d., $\gamma - \alpha$=high; pleochroism, X=yellow (somewhat greenish), Y=yellowish orange, Z=yellowish brown. These properties correspond to the 75% acmite phase in the diopside-acmite system. Further, it may be mentioned that the outer zone of the crystal is supposed to be of lower acmite content (40% or thereabouts) from its extinction angle $Z \wedge c \fallingdotseq 65°$. X-ray data are shown in Table 4. They approximately consist with

Fig. 1. Diopside stone in alkali-less glass. ×2.

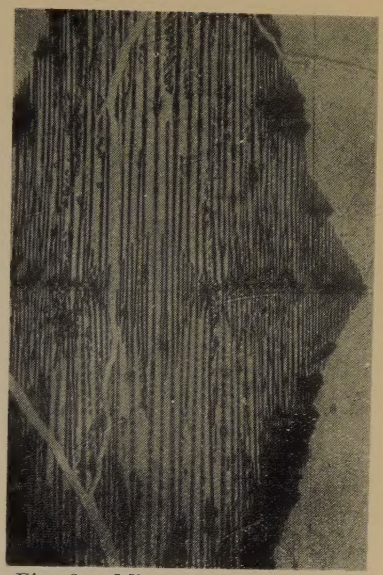

Fig. 2. Microphotograph of the (101) section of diopside stone showing the internal skeletal structure. Polarizer only, ×20.

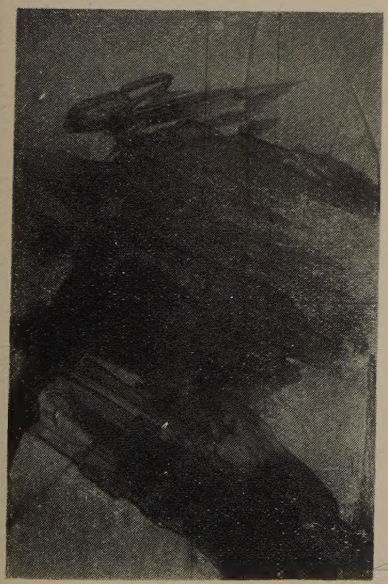

Fig. 3. Microphotograph of diopside-rich aegirine stone with inclusions of iron and magnetite. Polarizer only, ×40.

Fig. 4. Microphotograph of acmite-rich aegirine stone with inclusions of hematite. Polarizer only, ×40.

Fig. 5. Microphotograph of synthetic aegirine crystals. Polarizer only, ×50.

Fig. 6. Microphotograph of nepheline stone from fireclay refractory. Crossed nicols, ×30.

Fig. 7. Microphotograph of nepheline stone from electrofused high-aluminous refractory. Accessary minerals are corundum and carnegieite. Crossed nicols, ×25

Fig. 8. Microphotograph of nepheline stone from electrofused zirconia refractory. Polarizer only, ×25.

Table 4. X-ray powder data for the acmite-rich aegirine stone.

Aegirine stone		Acmite A. S. T. M. Card No. 3-0621	
I	*d*(Å)	*I*	*d*(Å)
50	3.677*	7	3.64
60	2.993	100	2.99
60	2.931	40	2.91
100	2.698*		
80	2.529	60	2.54
80	2.515*		
68	2.495	27	2.48
40	2.206*	20	2.20
28	2.127	20	2.12
40	2.104		
30	2.040 2.027**	20	2.03
		7	1.98
		7	1.93
60	1.845*		
50	1.696 1.690*	13	1.73
40	1.678	7	1.68
30	1.664	7	1.66
25	1.626	7	1.63
25	1.618	7	1.61
		7	1.54
28	1.519	13	1.51
55	1.488*	7	1.47
40	1.455*		
35	1.407	13	1.40
32	1.384	7	1.38
		7	1.33
35	1.302	7	1.30
35	1.275	7	1.27

* Diffraction lines of Fe_2O_3. ** Diffraction line of Fe.

the data of A. S. T. M. Index Card No. 3-0621 (acmite); and they contain some of the diffraction lines of hematite.

Discussion on the geneses of pyroxene stones

The thermal behaviors of the pyroxene stones were examined for the sake of clarifying their geneses. The procedure of heating test was as follows: A fraction of the glass containing the stone was placed on a piece of platinum plate and heated in a Silit electric furnace. At the beginning of each step the temperature of the furnace was elevated by 10°C. and kept for 30 min.. Then the test piece was removed from the furnace onto an iron plate to be quenched, and observed under the microscope. Thus the temperature at which the stone crystal had just dissolved into the surrounding glass was obtained. Furthermore the resultant glass was annealed at the rate of 20°C./hr. from the vitrifying temperature to somewhat lower one, and was observed if any crystal had formed. The results of these experiments are given below.

The test piece of diopside stone remained unchanged up to 1020°C., but a large number of diopside crystallites grew in the surrounding glass of the stone in the temperature range of 1020°C. to 1180°C.. Above 1180°C. these crystallites began to vitrify, and further the original diopside crystal also vitrified completely at temperatures exceeding 1200°C.. When the resultant glass was annealed from 1220° to 1180°C., an envelope-like shaped crystal similar to the original one has crystallized.

In the case of diopside-rich aegirine, all the crystals including no iron oxide began to dissolve into the surrounding glass at 1040°C., and completely dissolved at 1080°C. producing yellow glass; as for the crystals including some grains of iron oxide, dissolution began at 1060°C. and completed at 1100°C.. When the resultant yellow glasses were annealed, acmite-rich aegirine crystals formed instead of expected grass green phases similar to those of the original stone.

Acmite-rich aegirine began to dissolve into the surrounding glass at 1000～1020°C., and completely dissolved at 1080°C. producing yellow

glass. From this yellow glass, the same aegirine as original one has crystallized after heating at 1000°C. for an hour.

According to the above examination, the crystallization processes of pyroxene stones are implied as follows: The pyroxene stones have been formed by devitrification due to the shock caused by the fragments of iron or iron oxides, which accidentally dropped into the molten glass, on the cooling stage of the glass, while the aegirine stones have been formed in consequence of dissolution of iron oxide into the molten glass. The temperatures of crystallization are respectively about 1200°C. for the diopside stone, 1040°~1100°C. for the diopside-rich aegirine stone, and 1000°~1080°C. for the acmite-rich aegirine stone; thus they are all supposed to have formed in the working area of the tank furnace.

As for diopside stone, it does not occur so frequently in the soda-lime-silica glass and since, according to H. R. Swift[15], the chemical and thermal conditions for crystallization of diopside in glass are confined within narrow limits, it is believed that the proper condition for the growth of the exceptionally large crystals, found by the author, was the particular ratios of MgO and CaO contained in the mother glass.

Whether the composition of aegirine stones is diopside-rich or acmite-rich depends on the original state of the mother glass, location of dropping of iron fragments, and consequent degree of dissolution of iron into the glass. Thus the acmite-rich aegirine was formed only when hematite fragments had almost completely dissolved into the molten glass.

In order to ascertain the validity of this interpretation, synthesis of aegirine was carried out. A proper amount of chemically pure ferric oxide was placed on a fragment of soda-lime-silica glass in a platinum boat, and they were heated in the electric furnace. The heating product at above 1080°C. was the yellow glass, from which aegirine was crystallized by annealing. The crystals of the aegirine were long prismatic consisting of the major faces of (110), ($\bar{1}$01) and

($\bar{2}01$), and of the minute faces of (010) and (100) as shown in Fig. 5 (Plate II). Results of measurement of interfacial angles under the microscope with universal stage are: $110 \wedge \bar{1}10 \fallingdotseq 93°$ (E. S. Dana: 92° 50′), $100 \wedge 110 \fallingdotseq 45°$ (ditto: 46°25′), $\bar{1}00 \wedge \bar{1}01 \fallingdotseq 75°$ (ditto: 74°30′) and $\bar{1}00 \wedge \bar{2}01 \fallingdotseq 47°$ (calc.: 51°30′). Hourglass structure was observed. Optical properties are: $X \wedge c = -10° \pm 1°$, Y=b; $(-)2V = 71° \pm 2°$; $\alpha = 1.748 \pm 0.002$, $\beta > 1.76$, birefringence high; pleochroism, X=pale greenish yellow, Y=pale yellowish orange, Z=pale yellowish brown. These properties correspond to the 65~70% phase in the diopside-acmite system.

Properties of the stones produced from refractories

With the progress of the reaction between alumino-silicate refractories and molten soda-lime-silica glass in a tank furnace, nepheline and secondary corundum, which were not present in the original refractories, usually grow on the surface of refractories exposed to the action of molten glass. If, however, the reaction proceeds under unusual physico-chemical conditions, unusual minerals, i. e. albite, celsian, β-alumina, hercynite, spinel, and so on, may occur instead of or associating with nepheline and corundum. If these reaction products are torn off from the surface of refractories by the molten glass in which they incompletely dissolve, they may be carried as stones into the finished ware.

(1) *Nepheline stone* Nepheline is one of the most popular stones and has been described in a large number of papers. The properties of nepheline stones observed from the mineralogical point of view by the author are given below.

During exposure to attack of glass or sodic materials at about 1200°C., fireclay refractories produce the surface layer consisting of hexagonal short prismatic crystals of nepheline with lengths up to 0.7 mm. (Fig. 6, Plate II). Since these products occur in the refining or working area in which the refractories are used, once they are caught by the molten glass they will remain as stones in the finished

ware because of difficulty of their complete dissolution into the glass.

Table 5. X-ray powder data for the nepheline stones.

Nepheline stones				Nepheline A. S. T. M. Card No. 3-0613	
hexagonal short prisms		skeletons			
I	*d*(Å)	*I*	*d*(Å)	*I*	*d*(Å)
20	5.00				
50	4.32	40	4.33	3	4.34
100	4.18	85	4.20	20	4.16
				13	4.00
95	3.85	65	3.85	93	3.82
				10	3.62
82	3.267	75	3.278	25	3.25
				63	3.17
90	3.008	100	3.008	100	3.00
68	2.880	50	2.884	20	2.88
30	2.571	52	2.580	13	2.56
20	2.495	20	±2.495		
15	2.395	30	±2.399	5	2.39
53	2.341	65	2.345	20	2.34
46	2.304	32	2.309	10	2.30
8	2.120			5	2.12
33	2.090	25	2.094	15	2.08
8	±2.032	15	2.032		
15	1.982			3	1.98
15	1.929	15	1.933	10	1.92
8	1.883 1.881	15	1.886	8	1.88
5	1.838			3	1.83
		10	±1.817		
8	1.792 1.790	15	1.795 1.792	3	1.79
5	1.709 1.705				
10	1.693	12	1.695	1	1.70
9	1.634				
16	1.616	32	1.618	8	1.61
9	1.598				
30	1.561	60	1.561	23	1.56
				3	1.52
9	1.469	10	1.472	A. S. T. M. Card No. 2-0638	
8	1.456				
15	1.429	10	1.428	60	1.43
15	1.395			80	1.39
25	1.384	20	1.384	40	1.38
				40	1.35
8	1.342			20	1.33
9	1.314	15	1.315	40	1.32
10	1.279	15	1.281	70	1.28

Their optical properties are: colourless; uniaxial negative or anomalously biaxial with $(-)2V=8°\sim13°$; indices vary in the range of $\omega=1.535\pm0.0005$, $\varepsilon=1.531\pm0.0005$ to $\omega=1.544\pm0.0005$, $\varepsilon=1.540\pm0.0005$; $\omega-\varepsilon\fallingdotseq0.004$. X-ray powder data, as shown in Table 5, coincide with the data of natural nepheline except the line for $d=3.17$Å.

On the other hand, the nepheline stones originating from electrofused high aluminous or zirconia refractories are of feathery skeletons (Fig. 7, Plate II) or of skeletons showing hexagonal symmetry (Fig. 8, Plate II). They are occasionally associated with carnegieite or contain the pseudomorph after carnegieite, and usually include corundum or baddeleyite which were the constituent minerals of original refractories. The optical properties of this type of nepheline are: usually faint brown; uniaxial negative but occasionally biaxial with small optical angle, $\omega=1.531\sim1.537$, $\varepsilon=1.527\sim1.532$, $\omega-\varepsilon\fallingdotseq0.004$. X-ray powder data are given in Table 5.

(2) *High-albite* Though high-albite has never been found as stone in glass by the author, it was found in fireclay refractories as a result of glass attack against them and it may be possible to form a stone[4]. In the glass furnace, high-albite occurs instead of nepheline when the temperature is kept at 900°∼1000°C. for a long time or under some special condition. One of the examples of the former case is the occurrence of high-albite on the surface of refractories in contact with the molten glass at the working-end of the tank furnace, and of the latter is the product of reaction between glass and bottom bricks through the mineralizing action of copper oxide which deposited accidentally on the bottom of the melting area. The high-albites which grow on the surface of the working-end refractories have possibility of forming stones.

(3) *Celsian stone* Celsian stones were once found in a BaO-bearing glass of which the composition is shown in Table 1. They originated from the fireclay refractories attacked by the molten glass in the working area at about 1200°C..

Celsian crystals in the stones as well as those on the surface of

the refractories are monoclinic thin plates with diameter of 0.05～0.07 mm. (Fig. 9, Plate III). The face of the thin plate is probably (010); if it is the case, another faces will be supposed to be (100), (001), ($\bar{1}$01) and ($\bar{2}$01). The complex lamellar twinning or wave extinction was observed on some of the crystals.

It was very difficult to measure the optical constants of these crystals, but the outline was obtained: colourless; biaxial positive, (+) $2V=70°$～$80°$; mean value of indices was found to range between 1.588 and 1.597; birefringence is small. X-ray powder data are given in Table 6. Since the separation of the crystals from the surround-

Table 6. X-ray powder data for the celsian stone.

Celsian stone		Celsian A. S. T. M. Card No. 3-0850	
I	d(Å)	I	d(Å)
100	6.41	50	6.39
60	5.01		
60	4.53 4.49	25	4.52
35	3.83	25	3.84
40	3.576	25	3.58
95	3.442	50	3.45
100	3.280	50	3.29
50	3.076	25	3.01
40	2.946 2.931	25	2.94
70	2.764	25	2.75
		100	2.57
45	2.465	25	2.48
		50	2.32
		25	2.21
45	2.151	25	2.15
55	2.076	75	2.09
45	1.982	50	1.99
		50	1.93
		50	1.85
		75	1.79
25	1.670	50	1.68
20	1.642	50	1.64
20	1.577	60	1.58
		60	1.53
		60	1.50
45	1.434 1.410	60 50	1.46 1.42
40	1.325	50	1.32
		50	1.29
20	1.265	50	1.26

ing glass was poorly performed, the intensities of the lines obtained were very weak, but the main diffraction lines of celsian were recognized.

(4) *Corundum stone* The corundum stones, which have been frequently reported, mostly consist of the constituent corundums of electrofused high-aluminous refractories from which they separated into the molten glass. In this paper, the properties of the secondary corundum which originated from the corroded refractories will be described. The corundum crystals of this type are of hexagonal thin plates with diameter of 0.03~0.2 mm. as shown in Figs. 10 and 11 (Plate III). The source of the crystals shown in Fig. 10, being associated with nepheline, is a fireclay refractory attacked by the molten glass or alkali vapor at about 1200°C.. On the other hand, the crystals shown in Fig. 11, including baddeleyite grains, originate from an electrofused zirconia refractory in contact with the molten glass at a higher temperature of 1400°~1500°C.; their crystal habit differs from that of the corundum which is present in the original refractory.

The crystal faces are *c* and *m*. Optical properties are: uniaxial negative; colourless and $\omega=1.767\pm0.002$, $\varepsilon=1.759\pm0.002$ for the crystal shown in Fig. 10; colourless or pale yellow and $\omega=1.768\pm0.002$, $\varepsilon=1.760\pm0.002$ for the crystal shown in Fig. 11; birefringence $\omega-\varepsilon\fallingdotseq 0.008$ for both crystals.

X-ray powder pattern of the crystal shown in Fig. 10 consists with that of α-alumina (Table 7). As it was difficult to provide the corundum stones themselves for X-ray examination, a thin section of the corundum layer which developed on the surface of a fireclay refractory was used as the test piece.

The hexagonal thin plate crystals which occurred on the surface of fireclay refractories were once identified with β-alumina by L. Bor[1] and with corundum by some other authors without any optical or X-ray data. The results obtained by the present writer support the latter identification.

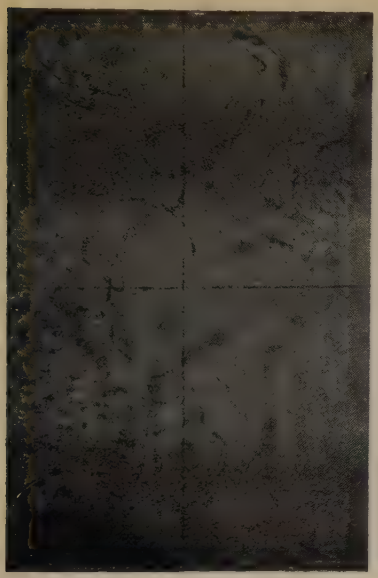

Fig. 9. Microphotograph of celsian stone. Polarizer only, ×170.

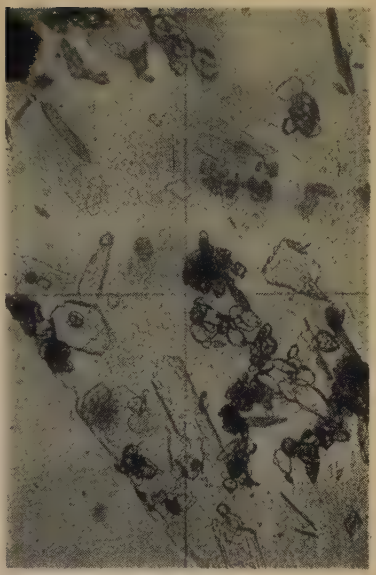

Fig. 10. Microphotograph of hexagonal thin plates of corundum embedded in nepheline. Polarizer only, ×60.

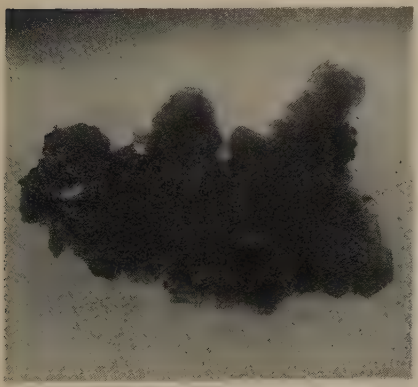

Fig. 11. Microphotograph of hexagonal thin plates of corundum including baddeleyite grains. Polarizer only, ×25.

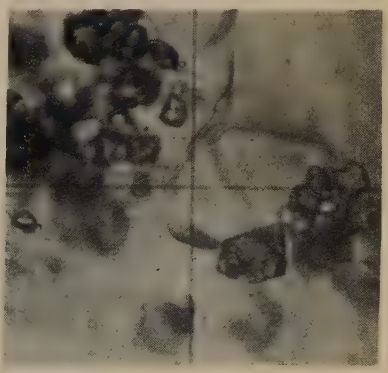

Fig. 12. Microphotograph of octahedral crystals of hercynite included in nepheline. Polarizer only, ×310.

Fig. 13. Microphotograph of spinel stone. Polarizer only, ×40.

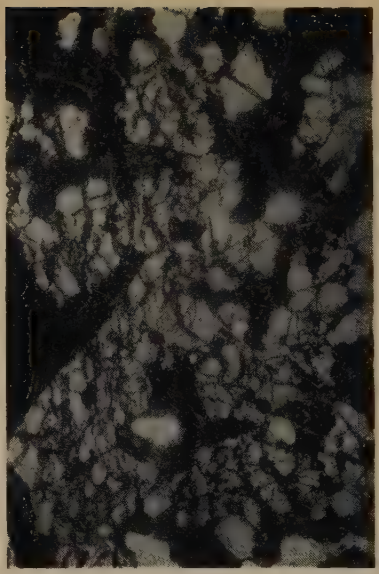

Fig. 14. Microphotograph of spinel on the surface of electrofused zirconia refractory. Inclusions are baddeleyite grains and nepheline skeletons. Polarizer only, ×25.

Table 7. X-ray powder data for the hexagonal thin plate crystals of corundum.

Hexagonal thin plates		α-alumina*	
I	*d*(Å)	*I*	*d*(Å)
20	3.453	0.8	3.47
23	2.547	0.9	2.55
15	2.368	0.8	2.375
		0.1	2.160
100	2.081	1.0	2.083
		0.1	1.96
10	1.739	0.8	1.736
35	1.602	1.0	1.598
		0.2	1.545
		0.4	1.508
25	1.403	0.7	1.401
35	1.374	1.0	1.371
8	1.336	0.1	1.33
8	1.276	0.1	1.271

* T. Kubo and S. Kato: "Chemical Analysis by X-ray diffraction" Nikkan Kogyo Shimbun Co. (1955) (in Japanese)

(5) *Hercynite stone* Hercynite stones were seldom found in soda-lime-silica glass, and their source was a fireclay refractory used as the wall above the glass level at the lower temperature position of a tank furnace. The surface of this refractory was contaminated with iron oxide which emanated from heating burners.

Hercynite crystals in the stone are yellowish brown octahedron with diameters about 0.005 mm. and are included in nepheline (Fig. 12, Plate III). Hercynite crystals which occurred on the surface of refractory were found scattering in the nepheline layer sandwiched in between the colourless glass, which covered the body of the refractory and contained thin plates of corundum, and the surface yellow glass containing cubes of magnetite.

The optical property is isometric and the refractive index is higher than 1.78. X-ray powder diffraction lines separated from

Table 8. X-ray powder data for the hercynite stone.

Hercynite stone			Hercynite A. S. T. M. Card No. 3-0894	
I	*d*(Å)	*hkl*	*I*	*d*(Å)
100	2.886	220	60	2.87
28	2.460	311	100	2.45
35	2.043	400	80	2.02
22	1.886	331		
		422	16	1.64
45	1.562	333	40	1.56
25	1.439	440	80	1.43
20	1.372	531		

those of associating nepheline were given in Table 8. The values of *d*(Å) are rather higher than those given in A. S. T. M. Card No. 3-0894, so it seems that this hercynite is a solid-solution containing more iron than the typical hercynite.

(6) *Spinel stone* Spinel is also one of the rare stones, and its source was an electrofused zirconia refractory used as the side wall near the entrance of the melting area of the soda-lime-silica glass tank furnace. The surface of the refractory had been exposed to scattering of batch materials at 1500°~1600°C.. The constituent corundum of this refractory produced spinel by the reaction with dolomite, and produced nepheline, β-alumina, and secondary corundum by the reaction with sodic materials.

Spinel stones are rounded grains, as shown in Fig. 13 (Plate IV), with diameter of about 0.5~0.7 mm., and associated with the feather aggregates of nepheline; spinel crystals found on the surface of the refractory are cubes or octahedrons with edges of 0.3~1 mm. and include baddeleyite and nepheline as shown in Fig. 14 (Plate IV). The spinels of both types are optically isometric, $n=1.723\pm0.001$, and colourless or pale yellow. X-ray powder method could not be applied to the spinel stones because of their small amounts. X-ray data obtained from the surface products of the refractory are given in

Table 9. X-ray powder data for the spinel on the surface of a refractory.

Spinel on the surface of a refractory			Spinel A. S. T. M. Card No. 5-0672	
I	*d*(Å)	*hkl*	*I*	*d*(Å)
35	4.69	111	4	4.67
100	2.851	220	40	2.858
65	2.436	311	100	2.436
		222	3	2.333
35	2.016	400	58	2.021
25	1.647	422	10	1.649
35	1.568	511	45	1.555
25	1.426	440	58	1.429

Table 9. The diffraction lines in the Table are the remainders after eliminating the lines for nepheline and baddeleyite from the data as they were obtained. They coincide with those of spinel except some disagreements of intensities owing to overlapping of some of the lines with those of baddelyite.

Discussion on the geneses of the stones from refractories

It is well-known that corundum occurs as the result of decomposition of mullite in almino-silicate refractories, and that nepheline occurs as a product of reaction between corundum and soda-lime-silica glass or sodic materials i. e. sodium carbonate or sulfate and soda vapor. These occurrences are clearly seen on a section of the surface zone of a used fireclay refractory. The temperatures at which corundum and nepheline are formed are considerably lowered from those given in the phase diagrams by the action of various fluxes which exist in the glass tank furnaces.

Nepheline crystals grow up to a cosiderable size on the surface of fireclay refractories used at the lower temperature (1200°C. or thereabouts) position, i. e. in the refining or working area of the tank furnace, and easily form stones when they enter the molten

glass.

On the other hand, during operation of the furnace the surface of electrofused high aluminous refractories is probably covered with the melt of nepheline composition, for these refractories are usually used in the melting area at higher temperature of 1400°~1600°C.. While the melt is caught in the flow of molten glass and carried into the lower temperature field, it may crystallize as skeletons capable of forming stones. Nepheline stones of this origin are occasionally associated with carnegieite or contain pseudomorphs after carnegieite because of higher temperature of their source than the inversion temperature (1248°C.) of carnegieite to nepheline.

As mentioned above, the crystallization temperature of nepheline is above 1200°C., and where temperature is kept at 900°~1000°C. high-albite occurs. An illustration is seen on the checker bricks in the regenerator of glass tank furnace; nepheline occurs on the surface of upper checkers subjected to higher temperature, and high-albite occurs on the surface of lower checkers exposed to lower temperature. Though it happens that high-albite, except those occurring at the working-end of the tank furnace, enters the molten glass, it will scarcely form stones because of its low melting temperature.

When BaO is contained in glass, celsian will be formed instead of nepheline. Though the temperature of the position where celsian has been formed is about 1200°C., according to the results of experiments in which fireclay refractories were dipped in the BaO-containing glass at various temperatures, celsian may grow best at 1400°C..

If Na_2O, Fe_2O_3, or MgO are added to the material of which, otherwise, corundum is to be formed, β-alumina, hercynite, or spinel may crystallize respectively. β-alumina has never been found as stone, but its occurrence on the surface of refractories leaves the possibility for it to form stones. The source of hercynite stones is the fireclay refractory used in the working area at about 1100°~1200°C.. If the surface of the refractory is contaminated with iron

oxide, hercynite will be formed as a reaction product between iron oxide and secondary corundum from the refractory. A sort of this occurrence was once reported by K. E. Seal[12]. According to the phase equilibrium diagrams of the iron oxide-Al_2O_3-SiO_2 system[9) 10)], hercynite may occur at considerably lower temperatures under low partial pressures of oxygen.

Spinel was found as a reaction product between corundum in the high-aluminous refractories and dolomite in the batch materials at the temperature of 1500°~1600°C.. There is no discrepancy between this occurrence and the crystallization courses of spinel in the phase diagram of the MgO-Al_2O_3-SiO_2 system. Since the spinel has its source near the entrance of the furnace, it has to go through a long way of high temperature exposed to active fluxes to remain as stones in the finished ware. This may be the cause of rare occurrence of spinel stones.

Acknowledgements

The author wishes to make grateful acknowledgements to the Emeritus Professor T. Ito of the Mineralogical Institute, University of Tokyo, Professor R. Sadanaga and Assistant Professor T. Shoda of the same institute, and Assistant Professor H. Minato of College of General Education, University of Tokyo, for their kind encouragements and advices during the present investigation. Thanks are also due to Dr. B. Yoshiki and Dr. S. Uemura, the former Superintendents of the Research Laboratory, Asahi Glass Co., and Mr. S. Suetoshi, Superintendent of the same laboratory, for their pertinent guidances and stimulating discussions.

References

1) Bor, L.: Jour. Amer. Ceram. Soc., **33**, 375 (1950).
2) Clark, C. B.: Jour. Amer. Ceram. Soc., **29**, 25 (1946).
3) Fabianic, W. L.: Jour. Amer. Ceram. Soc., **27**, 330 (1944).
4) Fukui, T.: Reports of the Research Laboratory, Asahi Glass Co., VI

[1] 12 (1956), (in Japanese).
5) Holland, A. J. and E. Preston: Jour. Soc. Glass Tech., **21**, 395 (1937); **22**, 82 (1938).
6) Insley, H. and Van D. Fréchette: "Microscopy of Ceramics and Cements", Academic Press Inc., New York, 161-174 (1955).
7) Knight, M. A.; Glass Ind., **28**, 69 (1947).
8) Lyle, A. K.: Bull. Amer. Ceram. Soc., **31**, 240 (1952).
9) Muan, A. and C. L. Gee: Jour. Amer. Ceram. Soc., **39**, 207 (1956).
10) Muan, A.: Jour. Amer. Ceram. Soc., **40**, 121, 420 (1957); Amer. Jour. Sci., **256**, 413 (1958).
11) Ostrovsky, I. A.: Miner. Abs., **10**, 464 (1949).
12) Seal, K. E.: Jour. Soc. Glass Tech., **32**, 46 (1948).
13) Swift, H. R.: Jour. Amer. Ceram. Soc., **30**, 165, 170 (1947).
14) Swift, H. R.: Glass Ind., **34**, 191 (1953).
15) Taylor, H. E. and D. K. Hill: "The Identification of Stones in Glass by Physical Method", The Glass Delegacy of the University of Sheffield (1952).
16) Winchell, A. N.: Amer. Jour. Sci., 5th Ser., **6**, 510 (1923).
17) Yagi, K.: Jour. Miner. Soc. Jap., **3**, 763 (1958), (in Japanese).
18) Yoder, Jr. H. S.: Amer. Jour. Sci., **248**, 225 (1950).

Manuscript received May 20, 1959.

Mineralogical Journal, Vol. 2, No. 6, pp. 375-396, Aug., 1959

VARIATION OF UNIT CELL PARAMETERS IN WOLFRAMITE SERIES

Akira Sasaki

Geological Survey of Japan

Abstract

The variation of unit cell parameters in the wolframite series has been investigated on the specimens synthesized by fusion of various mixtures of $FeCl_2 \cdot 4H_2O$, $MnCl_2 \cdot 4H_2O$ and $Na_2WO_4 \cdot 2H_2O$. The results show that a_0, b_0 and c_0 increase almost linearly with increasing MnO content as follows: from $a_0 = 4.732$Å, $b_0 = 5.707$Å and $c_0 = 4.965$Å in $FeWO_4$ to $a_0 = 4.834$Å, $b_0 = 5.758$ Å and $c_0 = 4.999$ Å in $MnWO_4$. Angle β varies also gradually from 90°00′ in $FeWO_4$ to 91°11′ in $MnWO_4$. However, it appears that the value of 90°00′ is maintained in the range from $FeWO_4$ to about $(Fe_{0.9}Mn_{0.1})WO_4$. The measurement has also been carried out on six natural specimens whose chemical data had been available. The unit cell parameters of these natural wolframites appear to follow the same variation diagram obtained with the synthetic specimens, although some numerical deviations are unavoidable. The differences between the result of chemical analysis and the composition determined by using the variation diagram are within the range of ±6 mol per cent.

Introduction

The wolframite series has generally been regarded to be a continuous solid solution composed of the two end members: ferrous tungstate and manganous tungstate. According to the molecular ratio of these two components, the series is commonly divided into the following three groups: ferberite (0 to 0.2 $MnWO_4$, 1.0 to 0.8 $FeWO_4$), wolframite (0.2 to 0.8 $MnWO_4$, 0.8 to 0.2 $FeWO_4$) and huebnerite (0.2 to 0 $FeWO_4$, 0.8 to 1.0 $MnWO_4$).

The crystal structure of this mineral series as well as some other groups of wolframate and molybdate were studied comprehensively by E. K. Broch[2]. According to him, a monoclinic unit cell

(P2/c) containing $(Fe, Mn)_2 (WO_4)_2$ and a similar atomic configuration is held for the whole series, though the details of the unit cell parameters vary with the iron to manganese ratio in the crystal. The following values were obtained for the three selected specimens.

	a_0	b_0	c_0	β
Artificial $FeWO_4$	4.70 Å	5.69 Å	4.93 Å	90°00′
Natural Wolframite $(Fe_{0.4}Mn_{0.6})WO_4$	4.78	5.73	4.98	90°26′
Artificial $MnWO_4$	4.84	5.76	4.97	90°53′

The gradual expansion of the unit cell volume and the increase in the angle β seem to correspond with increasing manganese content, and indicate the possibility of X-ray determination of the iron-manganese ratio in a given crystal. Moreover, if the iron end member has a pseudo-orthorhombic lattice with $\beta=90°$, as has been stated by Broch, the detail of the variation of β angle may also attract another interest.

Recently, K. Takano[11] measured the lattice parameters of this mineral series on some chemically analyzed natural specimens, and discussed briefly the relation between unit cell parameters and chemical composition.

As a part of their investigations on the thermal stability of this mineral, J. Berman and W. J. Campbell[1] carried out X-ray measurements on ten or more natural specimens including the synthetic two end members, and gave the diagrams which enable us to estimate the MnO content in the crystal by the variation of (200) or (030) spacing. The data also indicate that the angle β increases linearly with increasing manganese content, so that the value of 90° for the angle is confined only to the pure iron end member.

The purpose of the present investigation is to give further detail in the variation of unit cell parameters for the whole series, intending to make possible the rapid determination of iron-manganese ratio in any given crystal. In order to find the proper variation caused by iron-manganese ratio, pure $FeWO_4$-$MnWO_4$ series were

synthetically prepared and investigated. Measurements were also made on some natural specimens which had been chemically analyzed.

Experimental procedure

a) *Preparation of synthetic wolframites*

The synthetic wolframites for the present investigation were prepared by fusing sodium tungstate with various proportions of ferrous and manganous chlorides. The method is essentially the same as that described by A. Geuther and E. Forsberg[3]. The reagents used for the synthesis are listed below, with their guaranteed purity.

Sodium tungstate dihydrate ($Na_2WO_4 \cdot 2H_2O$)*:
WO_3, more than 69%; Mo, less than 0.01%.
Ferrous dichloride tetrahydrate ($FeCl_2 \cdot 4H_2O$)**:
$FeCl_2 \cdot 4H_2O$, more than 98%; Fe^{3+}, less than 0.1%.
Manganous dichloride tetrahydrate ($MnCl_2 \cdot 4H_2O$)**:
$MnCl_2 \cdot 4H_2O$, more than 98%; Fe, less than 0.002%.

The stoichiometrically weighed out components are fully hand-mixed in an agate mortar, heated in a porcelain crucible at about 800°C. for several minutes using electric furnace or Bunsen burner, and then cooled spontaneously. Because of such a rather rapid process in cooling, the resultant material is more or less porous cake of low crystallinity. However, under the binoculars, it is usually ascertained that the cake is composed of fine prismatic crystals, characteristic of this mineral. The cooled cake is roughly ground, and then washed repeatedly by hot water to remove any soluble impurity such as sodium chloride.

The colour of the powder varies with the composition of specimen from canary yellow in the manganese end member to nearly black in the iron end member, passing through reddish brown, brown and dark brown with increasing iron content. Purity of these final products are examined by X-ray powder method using Geiger-counter

* Prepared by Junsei Pure Chemicals Co. Ltd., Tokyo.
** Prepared by Muto Pure Chemicals Co. Ltd., Tokyo.

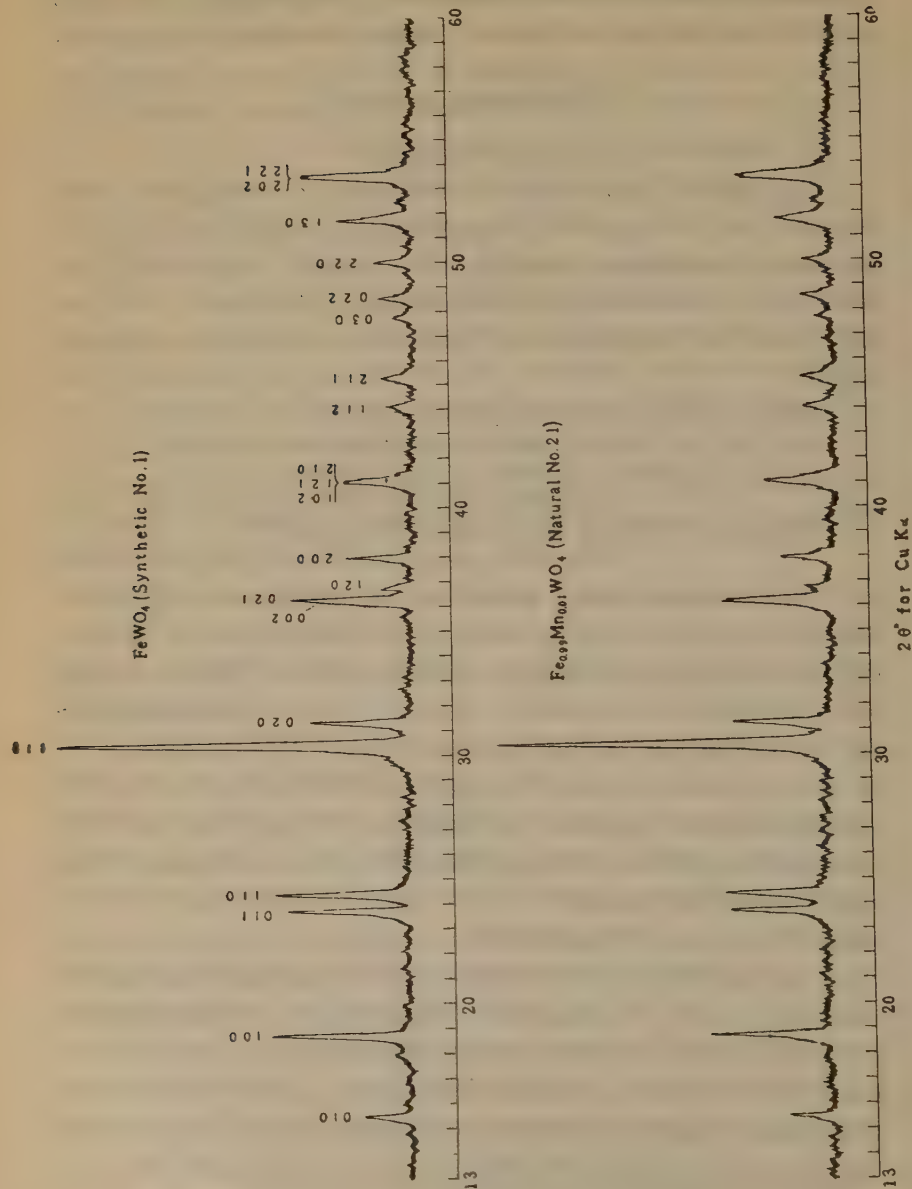

Fig. 1a. X-ray powder diffraction patterns of synthetic and natural ferberites.

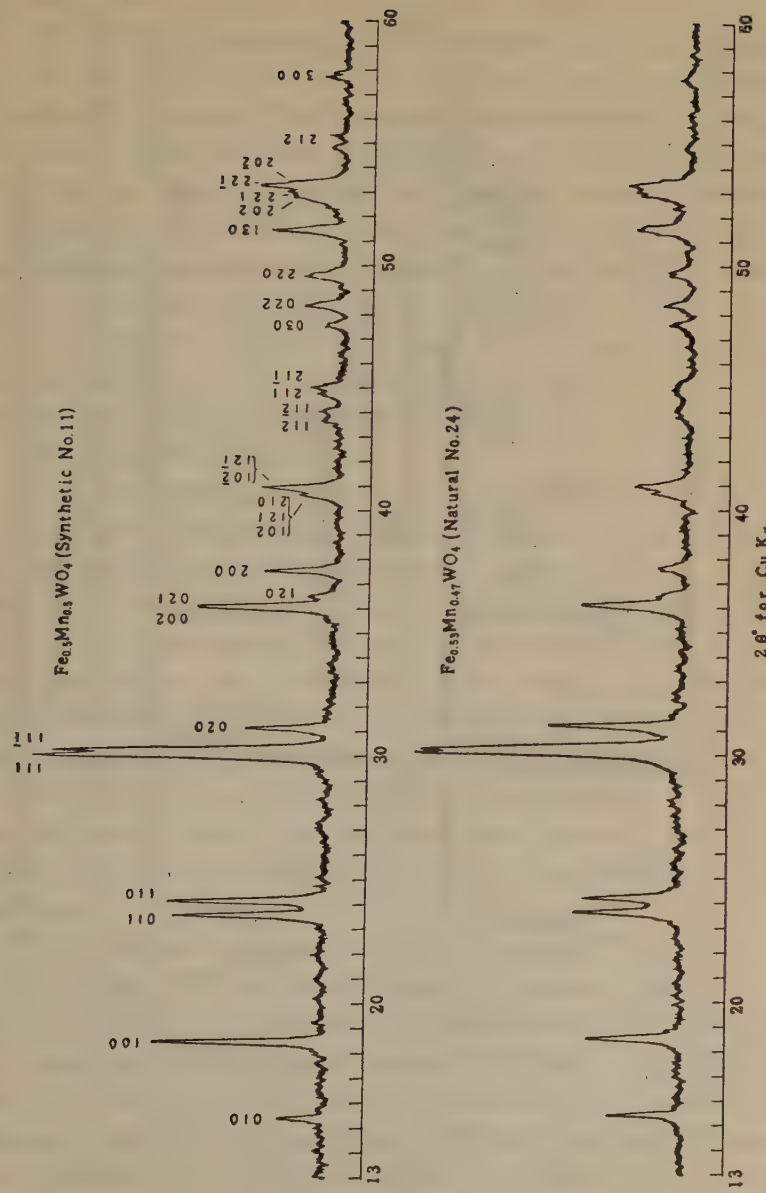

Fig. 1-b. X-ray powder diffraction patterns of synthetic and natural wolframites.

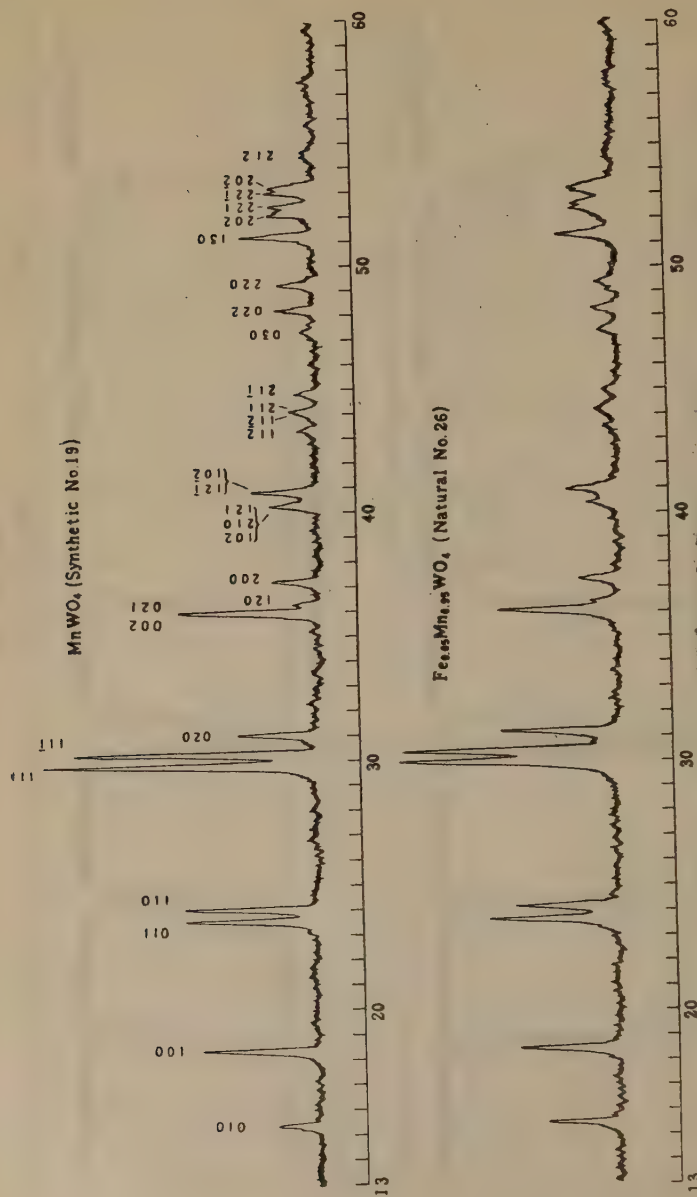

Fig. 1-c. X-ray powder diffraction patterns of synthetic and natural huebnerites.

diffractometer. In spite of such a simple method of synthesis, the X-ray diffraction patterns are always composed of sharp reflections which are quite identical with those of natural specimen practically free from impurities. For comparison, three representative patterns are shown in Fig. 1, together with those of the natural equivalents.

The syntheses were carried out for fifteen members of different composition, to cover the whole range of the series. The following compositions, expressed by the molecular ratio of $FeWO_4$ to $MnWO_4$, were synthesized as well as the two end members: 9/1, 6/1, 5/1, 4/1, 3/1, 2/1, 3/2, 1/1, 2/3, 1/2, 1/3, 1/6 and 1/9. In order to check the reproducibility of the syntheses, two independent runs were performed on several selected compositions.

b) *X-ray investigation*

The measurements were carried out on powders, mostly with a North American Phillipps' "Norelco" Geiger counter diffractometer, using unfiltered iron radiation ($\lambda=1.93597$ Å for $K_{\alpha 1}$) at 30 kV. and 10 mA., scanning speed 1° (2θ) in 4 minutes, chart speed 2 inches for 1° (2θ), time constant 8 seconds, angular aperture 1°, receiving slit 0.006 inches, and goniometer radius 170 mm.. Another similar type apparatus, Rigaku-Denki's "Geigerflex" was also used for some of the measurements, employing nickel-filtered copper radiation ($\lambda=1.54050$ Å for $K_{\alpha 1}$) at 30 kV. and 15 mA., scanning speed 1° (2θ) in 4 minutes, chart speed 4 cm. for 1° (2θ), time constant 8 seconds, angular aperture 1°, receiving slit 0.2 mm., and goniometer radius 185 mm..

The powdered specimen was packed in a slightly etched glass slide together with the internal standard silicon or quartz.

The unit cell parameters were essentially determined from the following sharp unambiguously indexed reflections: (011), (110), (111), ($11\bar{1}$) and (020). Each reflection as well as that of the standards were scanned repeatedly at least five times, and their mean 2θ values were adopted. Calibration was carried out based on the silicon's $a_0=5.4306_2$Å (at 21°C.) and the quartz's $a_0=4.9132_2$Å and $c_0=5.4049_0$Å

Table 1. X-ray powder diffraction data of Wolframites.

hkl	$FeWO_4$ (Spec. No. 1)				$Fe_{0.5}Mn_{0.5}WO_4$ (Spec. No. 11)				$MnWO_4$ (Spec. No. 19)				Intensity calculated by Broch
	$Q_{calc.}$	$Q_{obs.}$	$d_{obs.}$(Å)	I	$Q_{calc.}$	$Q_{obs.}$	$d_{obs.}$(Å)	I	$Q_{calc.}$	$Q_{obs.}$	$d_{obs.}$(Å)	I	
010	0.0307	0.0307	5.71	1.5	0.0304	0.0305	5.73	1.5	0.0302	0.0302	5.75	1.5	
100	0.0446	0.0446	4.736	4	0.0437	0.0438	4.780	6	0.0428	0.0428	4.831	4	3.5
011	0.0713	0.0713	3.745	3.5	0.0707	0.0707	3.761	5.5	0.0702	0.0703	3.770	4.5	3.8
110	0.0753	0.0753	3.644	3.5	0.0741	0.0741	3.673	5.5	0.0730	0.0730	3.700	4.5	3.3
111	0.1159	0.1157	2.940	10	0.1136	0.1135	2.968	10	0.1114	0.1115	2.995	10	10.0
$11\bar{1}$					0.1153	0.1152	2.946	9	0.1147	0.1148	2.951	8.5	10.0
020	0.1228	0.1226	2.856	2.5	0.1217	0.1219	2.864	3	0.1207	0.1207	2.879	2.5	2.4
002	0.1623	0.1625	2.481	2.5	0.1611	0.1616	2.488	4.5	0.1601	0.1605	2.496	5	4.0
021	0.1634	0.1634	2.474	3	0.1620				0.1607				4.6
120	0.1674	0.1676	2.443	1	0.1654	0.1652	2.460	1	0.1635	0.1637	2.471	1	0.8
200	0.1784	0.1784	2.367	1.5	0.1749	0.1748	2.392	2.5	0.1713	0.1713	2.415	1.5	3.7
012	0.1930				0.1915				0.1903				0.3
$10\bar{2}$	0.2069				0.2031				0.1996				1.4
$12\bar{1}$	0.2080	0.2077	2.194	2	0.2048	0.2034	2.217	1.5	0.2019	0.2004	2.234	1.5	0.8
210	0.2091				0.2053				0.2015				0.3
102					0.2065	0.2063	2.202	2.5	0.2063	0.2054	2.206	2	1.3
121					0.2065				0.2052				0.8
$11\bar{2}$	0.2376	0.2378	2.051	0.5	0.2335	0.2335	2.070	0.5	0.2298	0.2299	2.086	0.5	0.9
112					0.2369	0.2370	2.054	0.5	0.2365	0.2365	2.056	1	0.9
211	0.2497	0.2500	2.000	1	0.2439	0.2443	2.023	1	0.2382	0.2381	2.049	1	0.9
$21\bar{1}$					0.2473	0.2475	2.010	1	0.2449	0.2451	2.020	1	0.9

030	0.2763	0.2765	1.902	0.5	0.2738	0.2739	1.911	1	0.2715	0.2718	1.918	0.5	0.5
022	0.2851	0.2851	1.873	1	0.2828	0.2827	1.881	1.5	0.2808	0.2808	1.887	1.5	1.8
220	0.3012	0.3009	1.823	1	0.2966	0.2967	1.836	1.5	0.2920	0.2919	1.851	1.5	1.6
130	0.3209	0.3210	1.765	2	0.3175	0.3174	1.775	2.5	0.3143	0.3141	1.784	3	3.2
122	0.3297				0.3248				0.3203				0.3
122					0.3282				0.3270				0.3
202	0.3407				0.3326	0.3331	1.733	1.5	0.3248	0.3248	1.755	1.5	1.7
221	0.3418	0.3412	1.712	3	0.3351	0.3347	1.729	2	0.3287	0.3286	1.745	1.5	1.9
221					0.3385	0.3386	1.719	2.5	0.3354	0.3355	1.727	1.5	1.9
202					0.3393	0.3395	1.716	2	0.3382	0.3379	1.720	1.5	1.7
212	0.3714				0.3630	0.3631	1.659	0.5	0.3549	0.3546	1.679	0.5	
212					0.3698				0.3683				
300	0.4015				0.3935	0.3935	1.594	1	0.3855				
	$a_0=4.734$ Å $b_0=5.708$ $c_0=4.965$ $\beta=90°00'$				$a_0=4.783$ Å $b_0=5.733$ $c_0=4.983$ $\beta=90°35'$				$a_0=4.833$ Å $b_0=5.757$ $c_0=4.999$ $\beta=91°10'$				

Conditions: nickel-filtered copper radiation ($\lambda=1.54050$Å for $K\alpha_1$) at 30 kV. and 15 mA., scanning speed 1° (2θ) per minute, chart speed 1 cm. per minute, time constant 4 seconds, angular aperture 1°, receiving slit 0.2 mm., goniometer radius 185 mm..

(at 23°C.)*. The atmospheric temperature of laboratories where the measurements were carried out varied from 22°C. to 30°C..

Throughout the measurements, peak positions were read from the mid-point of the peak width at its two-thirds height, and the reading was reproducible at least to 0.005°(2θ), excepting (111) and ($11\bar{1}$) reflections in iron rich members. In the specimens containing more than about fifty per cent of $FeWO_4$ molecule, as is shown in Fig. 1, the separation between (111) and ($11\bar{1}$) is generally too small to be measured directly. In these cases each peak position was determined by comparing the peak broadness of (111)+($11\bar{1}$) with that of the nearest strong single reflection (020) at their two-thirds height, taking into account the effect of counting-loss phenomenon of the instrument[6) 9)], and assuming that the powders are sufficiently small to be considered to have no preferred orientation.

In order to verify the correctness of the procedure, calculated and observed Q values ranging from $2\theta=13°$ to 60° were also compared for the following three members, $FeWO_4$, $MnWO_4$ and $(Fe_{0.5}Mn_{0.5})WO_4$, whose powder diagrams have been taken with the scanning speed of 1°(2θ) per minute and the chart speed of 1 cm. per minute. The agreement between them appeared to be sufficient, as shown in Table 1.

The accuracy of the measurements is estimated as follows; ± 0.004 Å in a_0 and c_0, ± 0.003 Å in b_0, and $\pm 3'$ in β angle.

Unit cell parameters of wolframites

a) *Experimental results*

The X-ray measurements are summarized in Tables 2 and 3, and shown graphically in Figs. 2 and 3. Fig. 2 is a complete picture of the results, giving the variation pattern in the unit cell parameters of this mineral series with its iron-manganese ratio.

---

* These constants have been carefully determined by Dr. Iitaka of the University of Tokyo on the materials used here.

Table 2. Unit cell parameters of synthetic wolframites.

No.	$FeWO_4 : MnWO_4$ (molar)	a_0	b_0	c_0	β
1	1 : 0	4.734 Å	5.708 Å	4.965 Å	90°00′
2	1 : 0	4.730	5.707	4.965	90 00
3	9 : 1	4.742	5.711	4.969	90 00
4	6 : 1	4.747	5.714	4.970	90 05
5	5 : 1	4.750	5.716	4.972	90 07
6	4 : 1	4.752	5.718	4.974	90 12
7	3 : 1	4.759	5.719	4.975	90 18
8	3 : 1	4.755	5.719	4.973	90 14
9	2 : 1	4.766	5.723	4.977	90 22
10	3 : 2	4.772	5.726	4.978	90 27
11	1 : 1	4.783	5.733	4.983	90 35
12	1 : 1	4.780	5.729	4.981	90 34
13	2 : 3	4.794	5.739	4.987	90 43
14	1 : 2	4.797	5.741	4.985	90 49
15	1 : 3	4.811	5.746	4.990	90 53
16	1 : 3	4.807	5.746	4.992	90 53
17	1 : 6	4.816	5.750	4.993	91 00
18	1 : 9	4.825	5.755	4.997	91 03
19	0 : 1	4.833	5.757	4.999	91 10
20	0 : 1	4.835	5.758	4.999	91 12

Accuracy of the measurement is estimated as ± 0.004 Å for a_0 and c_0, ± 0.003 Å for b_0, and $\pm 0°03'$ for β.

The parameters a_0, b_0 and c_0 show smoothly increasing tendencies from iron to manganese end member, and each of their variation patterns, as shown in the figure, may be regarded to be essentially linear. The angle β of unit cell also increases with the increase of manganese content in the specimen. In this case, however, the variation diagram shows a rather peculiar feature that the increase of angle β from 90°00′ starts at the composition of $(Fe_{0.9}Mn_{0.1})WO_4$ instead of iron end member. However, any positive evidence indicating presence of symmetry change in the unit cell from monoclinic to orthorhombic could not be observed in the present experiments.

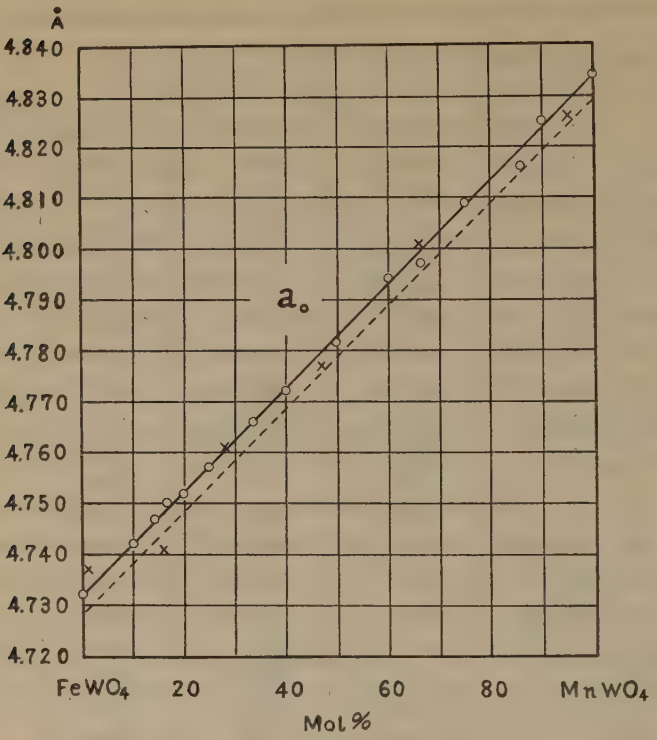

Fig. 2-a. Variation of a_0 in wolframite series. Circles represent synthetic specimens, while crosses natural specimens. Dashed line represents Berman-Campbell's result.

The variance in the separation of $(11\bar{1})$ and (111) reflections is so characteristic that it appears to be applicable for a simple determinative method of the iron-manganese ratio in the specimen. The difference between the spacings of the (011) and (110) reflections may also serve for the same purpose, because of their relatively close spacings and nearly equal intensities. The numerical values of the difference between those spacings are listed in Table 3, and graphically shown in Fig. 3a. For practical convenience, in Fig. 3b the same relations are illustrated in terms of 2θ angle when CuK_α or

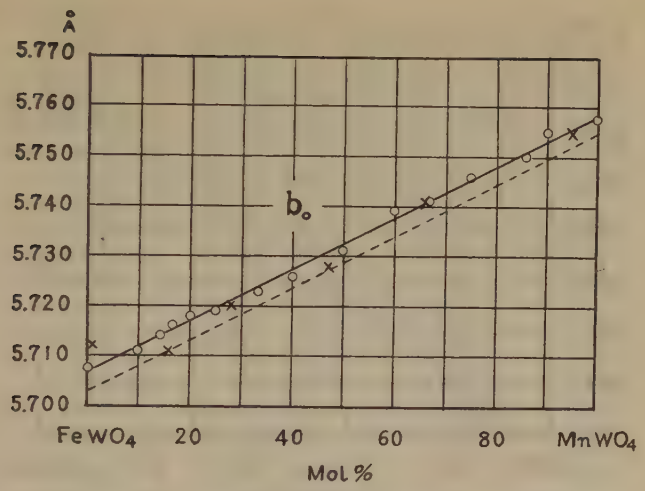

Fig. 2-b. Variation of b_0 in wolframite series. Circles represent synthetic specimens, while crosses natural specimens. Dashed line represents Berman-Campbell's result.

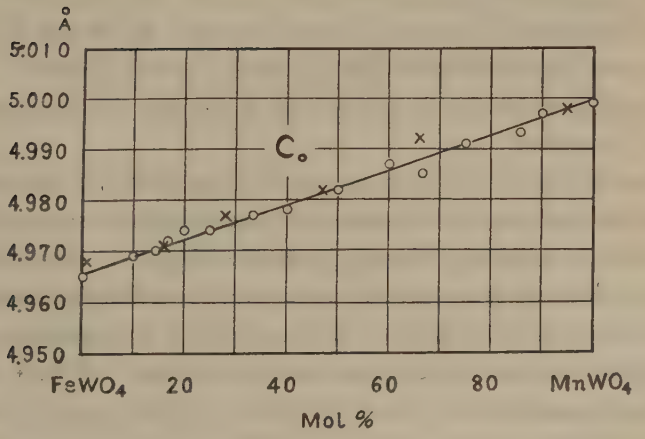

Fig. 2-c. Variation of c_0 in wolframite series. Circles represent synthetic specimens, while crosses natural specimens.

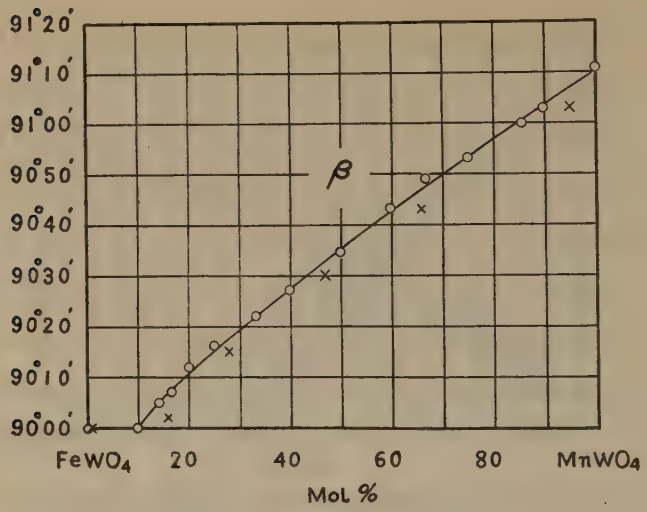

Fig. 2-d. Variation of angle β in wolframite series. Circles represent synthetic specimens, while crosses natural specimens.

FeK_α radiation is used.

For comparison of the present results, the previous data by Berman and Campbell are also plotted in Figs. 2a, 2b and 3b, where a_0 has been calculated from the d_{200} and β values given in Fig. 1 and Table 3, respectively, and b_0 from d_{030} in Fig. 2 of their paper[1].

b) *Discussion*

Since the synthetic wolframites were prepared in the form of poly-crystalline aggregates instead of single crystals, they might not always be composed of a single phase. However, the fairly good reproducibility in the synthetic procedure, as shown in Table 2, and the sharpness of the X-ray reflections which compares favourably with those of the natural specimens, as shown in Fig. 1, seem to clear up the ambiguity.

The variation diagrams of unit cell parameters obtained by the present writer through the investigation on artificial specimens are in good agreement with Berman-Campbell's results obtained for natu-

Table 3. Variations of $\Delta(d_{011}-d_{110})$ and $\Delta(d_{111}-d_{11\bar{1}})$ of synthetic wolframites, and their 2θ equivalents for CuK_α and FeK_α radiation.

No.	$\Delta(d_{011}-d_{110})$	$\Delta(2\theta_{110}-2\theta_{011})$		$\Delta(d_{111}-d_{11\bar{1}})$	$\Delta(2\theta_{11\bar{1}}-2\theta_{111})$	
		CuK_α	FeK_α		CuK_α	FeK_α
1	0.101_8 Å	$0.67_8°$	$0.85_7°$	0.000_0 Å	$0.00_0°$	$0.00_0°$
2	0.104_7	0.69_2	0.88_2	0.000_0	0.00_0	0.00_0
3	0.100_6	0.66_4	0.84_5	0.000_0	0.00_0	0.00_0
4	0.099_0	0.65_3	0.83_1	0.003_2	$0.0\bar{3}_5$	0.04_8
5	0.097_8	0.64_4	0.82_0	0.004_1	0.04_4	0.05_6
6	0.098_1	0.64_6	0.82_2	0.007_4	0.07_8	0.10_0
7	0.095_2	0.62_6	0.79_7	0.011_2	0.11_8	0.15_1
8	0.096_1	0.63_2	0.80_5	0.009_1	0.09_6	0.12_3
9	0.093_1	0.61_1	0.77_8	0.014_9	0.15_6	0.20_1
10	0.091_0	0.59_6	0.75_9	0.017_3	0.18_2	0.23_3
11	0.088_5	0.57_8	0.73_6	0.021_8	0.22_8	0.29_3
12	0.088_6	0.57_9	0.73_8	0.021_7	0.22_6	0.29_1
13	0.085_1	0.55_5	0.70_6	0.026_9	0.28_0	0.36_0
14	0.083_1	0.54_2	0.68_9	0.031_1	0.32_8	0.40_9
15	0.078_8	0.51_0	0.65_2	0.033_7	0.35_0	0.44_8
16	0.081_6	0.53_0	0.67_5	0.033_3	0.34_6	0.44_3
17	0.078_0	0.50_6	0.64_3	0.038_1	0.39_5	0.50_7
18	0.075_9	0.49_1	0.62_5	0.039_9	0.41_3	0.53_1
19	0.073_2	0.47_3	0.60_2	0.044_1	0.45_6	0.58_5
20	0.072_4	0.46_7	0.59_5	0.044_8	0.46_3	0.59_5

ral crystals, taking into account the accuracies in both investigations.

According to the present investigation the value of angle β remains at 90°00′ between $FeWO_4$ and $(Fe_{0.9}Mn_{0.1})WO_4$ at which, according to Berman-Campbell's results, the specimen should have the angle β of about 90°06′. Berman and Campbell obtained their conclusion from the variation diagram of $\Delta(2\theta_{11\bar{1}}-2\theta_{111})$ extrapolated below 40 mol per cent MnO, while the present writer has suffered much difficulties in reading the value of $\Delta(2\theta_{11\bar{1}}-2\theta_{111})$ in the X-ray reflection charts of iron rich members. Therefore, to verify the variation conclusively, it is desirable to utilize some instrument having more

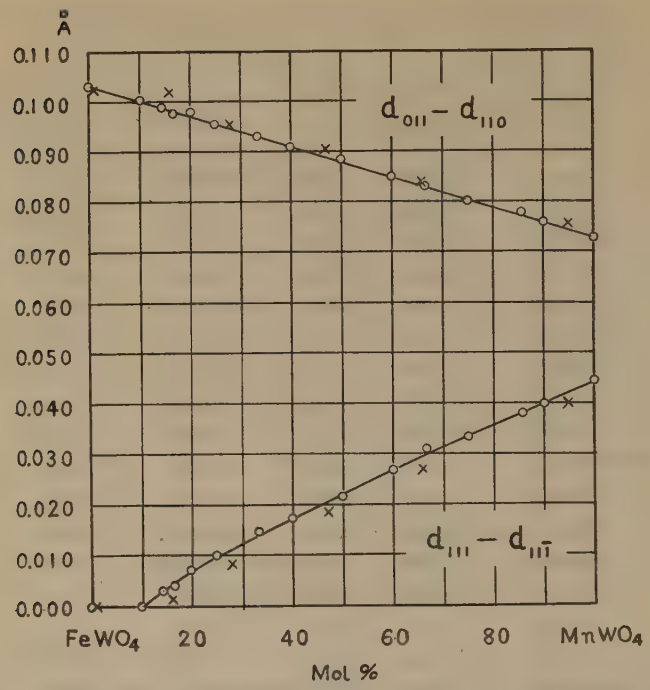

Fig. 3-a. Variations of $\Delta(d_{011}-d_{110})$ and $\Delta(d_{111}-d_{11\bar{1}})$ in wolframite series. Circles represent synthetic specimens, while crosses natural specimens.

enhanced resolving power, for example such as the Guinier camera or the diffractometer with curved crystal monochrometer.

Even though the angle β of the iron rich members is confirmed to be 90°00′, whether the symmetry change from monoclinic to orthorhombic is present or not is another problem, which should be examined by single crystal diffraction method.

Studies on Natural Wolframites

a) *Experimental*

In order to study the applicability of the diagrams in Fig. 2 for natural specimens, four Japanese wolframites, which had been sepa-

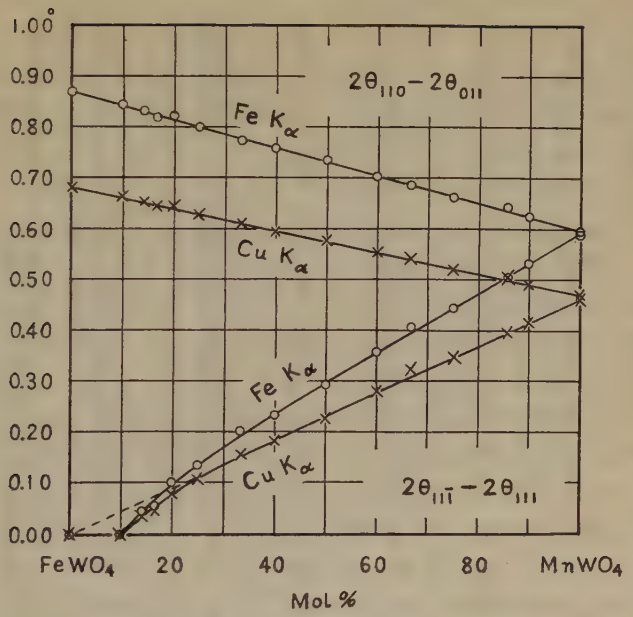

Fig. 3-b. Variations of $\Delta(2\theta_{110}-2\theta_{011})$ and $\Delta(2\theta_{11\bar{1}}-2\theta_{111})$ in wolframite series, when Cu K_α or Fe K_α radiation is used. Dashed line represents Berman-Campbell's result.

rated by a Frantz isodynamic separator and carefully hand-picked under the binoculars, were chemically analyzed and their unit cell parameters were determined. The chemical analyses were performed by H. Haramura of Tokyo Institute of Technology. The measurements of unit cell parameters were also made on two other specimens whose chemical data had been available. One is "reinite", a ferberite equivalent supposed to be a pseudomorph after scheelite, from the Otomé mine[7], and the other is a huebnerite from the Hagidaira mine[5].

The results are summarized in Tables 4 and 5, and also plotted in Figs. 2 and 3. As shown in Table 4, the valency of iron in wolframites was assumed to be wholly bivalent, although Berman and Campbell's results suggested that a small amount of ferric iron may

Table 4. Locality, mode of occurrence and chemical data of natural wolframites.

No.	Locality	Mode of occurrence	WO_3	MnO	FeO	Total	Calculated chemical formula**	Idealized chemical formula***
			%	%	%	%		
21	Otomé, Yamanashi Pref.	Plutonic type† W-quartz vein in hornb.-granite	75.21	0.19	24.37	99.77	$Fe_{1.03}Mn_{0.01}W_{0.99}O_4$	$Fe_{0.99}Mn_{0.01}WO_4$
22	Ebisu, Gifu Pref.	Plutonic type† Bi-W-quartz vein in quartz porphyry	73.47	3.68	22.60	99.75	$Fe_{0.96}Mn_{0.16}W_{0.96}O_4$	$Fe_{0.84}Mn_{0.16}WO_4$
23	Funai, Kanéuchi, Kyoto Pref.	Plutonic type† Sn-W-quartz vein in Palaeozoic sediments	75.84	6.52	17.48	99.84	$Fe_{0.74}Mn_{0.28}W_{0.99}O_4$	$Fe_{0.72}Mn_{0.28}WO_4$
24	Yomei, Kanéuchi, Kyoto Pref.	ditto	75.85	10.88	12.72	99.45	$Fe_{0.54}Mn_{0.47}W_{1.00}O_4$	$Fe_{0.53}Mn_{0.47}WO_4$
25	Gessei, Kanéuchi, Kyoto Pref.	ditto	75.68	15.29	8.43	99.40	$Fe_{0.36}Mn_{0.66}W_{0.99}O_4$	$Fe_{0.34}Mn_{0.66}WO_4$
26	Hagidaira, Gunma Pref.	Plutonic type† quartz vein passing through a bedded manganese deposit in Palaeozoic sediments	75.54	21.87	1.22	98.63*	$Fe_{0.05}Mn_{0.95}W_{1.00}O_4$	$Fe_{0.05}Mn_{0.95}WO_4$

Analyst: No. 21, by F. Kodera[7]; No. 22~25, by H. Haramura; No. 26, by K. Isono[5].

* 1.25% SiO_2 in addition.

** Based on O=4.

*** After Hess and Schaller's procedure[4].

† Includes pegmatitic to hypo- or mesothermal types[12].

Table 5. Unit cell parameters, $\Delta(d_{011}-d_{110})$, $\Delta(d_{111}-d_{11\bar{1}})$ and estimated chemical formulae of natural wolframites.

No.	a_0	b_0	c_0	β	$\Delta(d_{011}-d_{110})$	$\Delta(d_{111}-d_{11\bar{1}})$	Chemical formula determined on the basis of		
							Unit cell parameters*	$\Delta(d_{011}-d_{110})$	$\Delta(d_{111}-d_{11\bar{1}})$
21	4.737 Å	5.712 Å	4.968 Å	90°00′	0.102_5 Å	0.000_0 Å	$Fe_{0.93}Mn_{0.07}WO_4$	$Fe_{0.98}Mn_{0.02}WO_4$	
22	4.741	5.711	4.971	90 02	0.102_0	0.001_8	$Fe_{0.89}Mn_{0.11}WO_4$	$Fe_{0.96}Mn_{0.04}WO_4$	$Fe_{0.88}Mn_{0.12}WO_4$
23	4.761	5.720	4.977	90 15	0.095_5	0.008_8	$Fe_{0.72}Mn_{0.28}WO_4$	$Fe_{0.75}Mn_{0.25}WO_4$	$Fe_{0.78}Mn_{0.22}WO_4$
24	4.777	5.728	4.982	90 30	0.090_7	0.018_7	$Fe_{0.56}Mn_{0.44}WO_4$	$Fe_{0.58}Mn_{0.42}WO_4$	$Fe_{0.57}Mn_{0.43}WO_4$
25	4.801	5.741	4.992	90 43	0.084_0	0.027_0	$Fe_{0.32}Mn_{0.68}WO_4$	$Fe_{0.37}Mn_{0.63}WO_4$	$Fe_{0.40}Mn_{0.60}WO_4$
26	4.826	5.755	4.998	91 03	0.075_8	0.040_0	$Fe_{0.07}Mn_{0.93}WO_4$	$Fe_{0.09}Mn_{0.91}WO_4$	$Fe_{0.10}Mn_{0.90}WO_4$

* Average of the compositions determined by a_0, b_0, c_0 and β respectively.

be intrinsic for natural wolframites. To plot the results in Figs. 2 or 3, the chemical formula was idealized through the procedure described by Hess and Schaller[4], that is, the MnO content in the analytical data was used as the basis of calculation. The chemical compositions determined by the unit cell parameters, $\Delta(d_{011}-d_{110})$ and $\Delta(d_{111}-d_{11\bar{1}})$ respectively, were also given in Table 5 for comparison with the results obtained by wet chemical analysis in Table 4.

b) *Discussion*

As evident in Fig. 2, the variation of unit cell parameters in natural wolframites follows approximately that of synthetic specimens, although an intimate agreement could not be established. The average of the compositions of each sample determined by a_0, b_0, c_0 and β respectively (Table 5), shows fairly good agreement with the chemical analysis (Table 4) with the allowance of about ± 6 mol per cent. On the other hand, however, if the composition is determined by any one parameter,

the result will be sometimes unreliable. For example, the composition of specimen No. 25 determined by c_0 deviates from the result of chemical analysis by about 12 mol per cent.

In the variation diagram of $\Delta(d_{011}-d_{110})$ and $\Delta(d_{111}-d_{11\bar{1}})$ versus chemical composition (Fig. 3a), the points of natural specimens are mostly found close to the variation curves obtained with synthetic specimens. The deviation from the curves is generally less than 6 or 7 mol per cent, which is nearly equal to the accuracy of the composition determined by the unit cell parameters, although the composition read from the curves have general tendency to show less manganese content compared with the results of wet chemical analysis. The quick determination of composition depending on $\Delta(d_{011}-d_{110})$ and $\Delta(d_{111}-d_{11\bar{1}})$, therefore, appears to be useful again for natural specimens, in spite of its simplicity.

The cause of the small differences of the unit cell parameters between natural and synthetic wolframites as discussed above is not clear. At least, however, it may be partly originated in experimental errors in chemical analysis as well as X-ray measurement, and partly derived from the intrinsic character of natural specimen. The probable existence of the intrinsic trivalent iron in the wolframite crystals suggested by Berman and Campbell, is an important problem to be solved from the view-point of crystal chemistry. Moreover, the influence of commonly occurring impurities in this mineral, such as Nb, Ta, Sc, and some rare earths, may not be negligible, as has been partly revealed by the study of F. Leutwein[8].

Summary and conclusion

The variation of unit cell parameters in the wolframite series has been investigated on the specimens artificially prepared. The final results are compiled graphically in Fig. 2. All of a_0, b_0 and c_0 increase almost linearly with increasing manganese content. Among them, a_0 has the most predominant variation, and its variation range is about two times that of b_0 and three times that of c_0. Angle β

also increases with the increase of manganese, starting from 90°00′ in the iron end member. However, it seems to remain at 90°00′ from $FeWO_4$ to about $(Fe_{0.9}Mn_{0.1})WO_4$, although the conclusive decision is difficult because of the limitation of the experimental accuracy.

The investigation on natural specimens indicates that the estimation of iron-manganese ratio in natural wolframites by measuring the unit cell parameters is fairly reliable. The estimated ratio agrees with the result of chemical analysis with the allowance of ± 6 mol per cent. However, the reliability of this method should be finally examined by further investigations on many more natural specimens, considering the effects of intrinsic impurities to the unit cell parameters.

When the quick determination of approximate composition or the relative comparison among many specimens is wanted, the variation diagram of $\Delta(d_{011}-d_{110})$ and $\Delta(d_{111}-d_{11\bar{1}})$ in Fig. 3 may be convenient.

Rapid estimation of the iron-manganese ratio in wolframite without any destruction of the crystal lattice, is now also practicable in X-ray fluorescent analysis or in magnetic susceptibility measurement[10]. As compared with these methods, the X-ray diffraction procedure has an advantage that the measurement is not so disturbed by the presence of impurities in the specimen. However, the accuracy of estimation may become the highest in X-ray fluorescent analysis carried out with care.

Acknowledgements

This work was planned and partly carried out in the Geological Institute, University of Tokyo, and continued in the Geological Survey of Japan.

The author wishes to express his sincere gratitude to Prof. T. Watanabe of the University of Tokyo for his kind interests and stimulating advice on this work, and to Dr. T. Kimura and Mr. T. Hattori of the Geological Survey for giving various facilities. He

is also indebted to Prof. F. Leutwein in Germany for valuable suggestions, and to Prof. N. Katayama, Drs. Y. Iitaka and K. Doi of the University of Tokyo and Dr. Y. Shimazaki of the Geological Survey for their helpful discussions and criticism. His thanks are also due to Messrs. F. Hirowatari and H. Takeda of the Geological Survey for the specimen of huebnerite from the Hagidaira mine and the permission of using their unpublished chemical data on the specimen, and to Dr. T. Katsura and Mr. H. Haramura of the Tokyo Institute of Technology for chemical analyses of wolframites.

References

1) Berman, J. and W. J. Campbell: U. S. Bureau of Mines Rept. Invest. 5300 (1957).
2) Broch, E. K.: Norsk. Ak., Oslo, Math.-Nat. Kl., Skrifter, No. 8 (1929).
3) Geuther, A. and E. Forsberg: Ann. Chem. Pharm., **120**, 270 (1861).
4) Hess, F. L. and W. T. Schaller: U. S. Geol. Surv., Bull. No. 583, 40 (1914).
5) Hirowatari, F. and H. Takeda: Huebnerite from the Hagidaira mine, Gunma Prefecture (in prep.).
6) Iitaka, Y.: Jour. Miner. Soc. Japan, **3**, 244 (1957) (in Japanese).
7) Ito, T. and K. Sakurai: Wada's Minerals of Japan 3rd Edit., 360, Tokyo (1947).
8) Leutwein, F.: Freiberg. Forsch., Nr. 8, 8 (1951).
9) Peiser, H. S. et al.: "X-ray Diffraction by Polycrystalline Materials", Inst. Physics, London (1955).
10) Spokes, E. M. and D. R. Mitchell: Mining Eng., **10**, 373 (1958).
11) Takano, K.: Jour. Japanese Assoc. Miner. Petr. Econ. Geol., 41, 32 (1957) (in Japanese).
12) Watanabe, T. and A. Sasaki: Tin and tungsten deposits of Japan, Proc. 9th Pacific Sci. Cong. (1957) (in press).

Manuscript received June 1, 1959.

Mineralogical Journal, Vol. 2, No. 6, pp. 397-407, Aug., 1959

IKUNOLITE, A NEW BISMUTH MINERAL FROM THE IKUNO MINE, JAPAN

Akira Kato

Geological Institute, University of Tokyo

Abstract

Ikunolite, $Bi_4(S, Se)_3$, a new mineral from the Ikuno mine occurs in ferberite-bismuth-bismuthinite quartz vein. It belongs to rhombohedral system with $a_{rh}=13.28$ Å, $\alpha=18°00'$, $Z=1$ (or $a_0=4.15$ Å, $c_0=39.19$ Å, $Z=3$ in hexagonal lattice) and the space group is $R\bar{3}m$. Physical and optical properties are: lead grey in colour and dark grey in streak colour; hardness 2, very flexible; specific gravity=7.97 (calc.), 7.8 (meas.); perfect cleavage parallel to {0001}; anisotropic in the section diagonal to the basal cleavage and etched by HNO_3 and $FeCl_3$ solution. Chemical analysis gives $Bi_{3.79}(S_{2.76}Se_{0.24})_{3.00}$ close to $Bi_4(S, Se)_3$ with S: Se=92: 8. The sheet structure determined by single crystal method is closely related to the other rhombohedral chalcogenides of bismuth. Ikunolite resembles joseite A [Bi_4TeS_2] in structure, crystallography and optical properties and belongs to the same group of bismuth-chalcogenide minerals with Bi: (S, Se, Te)=4: 3.

Introduction

In 1957 during the course of a study of the mineral deposits of the Ikuno mine, a famous xenothermal deposit with copper, zinc, lead, tin, wolfram, gold and silver ores, the writer received a small specimen with ferberite, bismuth, bismuthinite and this mineral in a quartz vein from No. 6 south stope, 21st level (107 m. under sea level), Senju-maé vein of Kanagasé vein group from K. Horikawa of the Geological Section of the mine. The writer was also able to observe the occurrence of this mineral in the original locality.

The chemical properties and X-ray studies clarified this mineral to be a new species of the composition $Bi_4(S, Se)_3$ with rhombo-

hedral symmetry. The writer has called this mineral ikunolite after the locality name.

Occurrence and mineral association

The Ikuno mine is situated in the central part of Hyôgo prefecture. The ore deposits consist of about fourty veins cutting Miocene volcanic sediments and have complex mineral assemblages as the products of successive mineralization. The assemblage containing this mineral belongs to the product of the second stage of mineralization according to Takeo Kato[7], who observed four stages of mineralization in the Ikuno ore deposits.

The Senju-maé vein is one of the important lodes in this mine and is characterized by copper and zinc ores with small amount of tin. Ikunolite was discovered in the central part of a composite vein, which has rather exceptional mineral assemblage consisting of ferberite, bismuth minerals and quartz with sporadic cassiterite.

Ikunolite fringes native bismuth as well as bismuthinite, or forms platy mass with indefinite outline, attaining to a few millimeters in maximum diameter (Fig. 1, Plate I). Ferberite and quartz which are the major constituents of the ore occur also as minor inclusions in this mineral. X-ray spectrochemical analyses for the native bismuth and the bismuthinite disclosed the absense of any unusual constituents.

Chemical composition

Chemical analysis was kindly carried out by T. Katsura, Tokyo Institute of Technology, on a small amount of hand-picked material in which large amount of bismuth, small amount of selenium (less than 5%) and minor amounts of silver and tellurium (probably less than 0.1%) had been detected by the writer with X-ray spectroscopy. The result of the chemical analysis is given in Table 1.

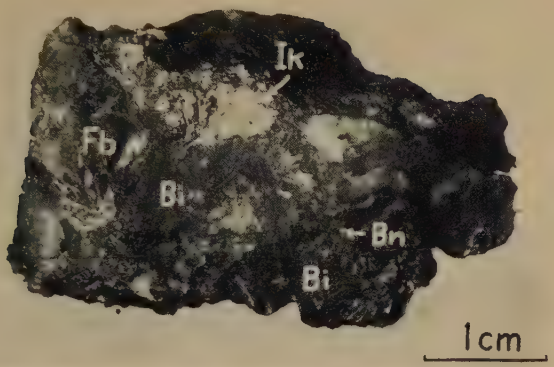

Fig. 1. Ikunolite (Ik) in ferberite (Fb)-bismuth (Bi)-bismuthinite (Bn)-quartz vein from the No. 6 south stope, 21st level, Senju-maé vein, Kanagasé vein group, Ikuno mine.

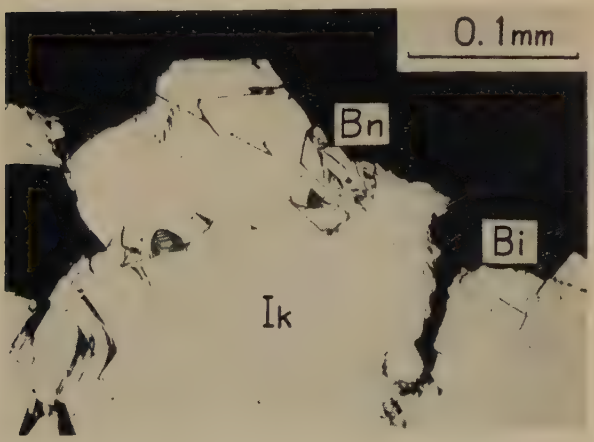

Fig. 2. Photomicrograph of polished section of ikunolite (Ik) associated with bismuth (Bi) and bismuthinite (Bn). Dark area is cementing material for polishing.

Table 1. Chemical composition of ikunolite.

	1	2	3
Bi	79.69 %	87.99%	88.67%
S	8.89	9.82	9.32
Se	1.98	2.19	2.01
Rem.	[9.44]		
Total	[100.00]%	100.00%	100.00%

1. Ikunolite from the No. 6 south stope, 21st level, Senju-maé vein, Kanagasé vein group, Ikuno mine. Remnants are ferberite and quartz.
2. Ikunolite, after deducting remnant.
3. Calculated as $Bi_{4.00}(S_{2.76}Se_{0.24})_{3.00}$.

After deducting remnant, the analysis gives the chemical formula of $Bi_{3.79}(S_{2.76}Se_{0.24})_{3.00}$ which is close to $Bi_4(S, Se)_3$ with S : Se = 92 : 8 or $Bi_{4.00}(S_{2.76}Se_{0.24})_{3.00}$, the composition being confirmed by structure analysis as will be described later.

Physical and optical properties

Physical and optical properties of this mineral are given in Table 2 with those of joseite A [Bi_4TeS_2] by Thompson[11]. There is striking resemblance between them.

X-ray studies

X-ray studies were carried out on the cleavage pieces and powdered material of ikunolite. The crystallographic orientation was easily determined by taking the cleavage plane as {0001}. Though the high flexibility of the mineral gave poor samples for X-ray studies, one of them gave a good pattern of D_{3d} in the Laue symmetry in the cleavage plane. From the oscillation photograph about the a-axis which had been determined by the Laue spots, a_0 was measured as 4.15 Å. The X-ray powder lines are given in Table 3 with those of joseite A and are indexed on the basis of the hexagonal unit

Table 2. Physical and optical properties of ikunolite and joseite A.

	Ikunolite	Joseite A
Crystal system	Rhombohedral	Rhombohedral
Colour	Lead grey	Silver white
Luster	Metallic	Metallic
Cleavage	Parallel to base, perfect	Parallel to base, perfect
Hardness	2, very flexible	2
Streak colour	Dary grey	
Specific gravity	7.97 (calc.) 7.8 (meas.)	8.10
Colour in polished section	White with faintly creamy tint	White
Polishing hardness	B (basal section) B- or A (diagonal section)	B (basal section) A (diagonal section)
Anisotropism	Nearly isotropic in basal section. Moderate in diagonal section; pale grey to grey	Nearly isotropic in basal section. Moderate in diagnal section; greenish grey to dark greenish grey
Extinction	Four times in perpendicular section to basal plane	
Etching by HNO_3 (1: 1)	Positive, stains bluish grey with dark brown fume.	Positive, effervesces and stains dark grey.
HNO_3 (conc.)	Positive, effervesces and stains grey with dark brown fume.	
HCl (1: 1)	Negative	Positive, stains light grey.
$FeCl_3$	Positive, stains brownish red.	Positive, stains pale bluish grey.
KOH	Nagative.	Nagative.
KCN	Nagative.	Nagative.
$HgCl_2$	Nagative.	Nagative.

Table 3. X-ray powder data for joseite A and ikunolite.

1.		2.				
d	*I*	*d*	*I*	Q_{obs}	Q_{calc}	*hkl*
		13.08 Å	5	0.006	0.006	003
		6.56	20	0.023	0.023	006
4.38 Å	20	4.34	50	0.053	0.053	009
3.61	20	3.536	20	0.0800	0.0800	102
3.07	100	3.022	100	0.1094	0.1095	017
2.57	20	2.527	10	0.1567	0.1567	10.11
2.24	50	2.205	30	0.2058	0.2050	10.14
2.11	50	2.076	20	0.2320	0.2322	110
2.05	10	2.026	5	0.2437	0.2441	01.16
1.967	10					
1.894	20	1.865	20	0.2876	0.2871	00.21
1.819	5	1.791	5b	0.3118	0.3112	022
1.779	5					
1.744	30	1.713	5b	0.3409	0.3415	207
1.654	10					
1.616	5					
1.537	30	1.513	10	0.4368	0.4372	02.14
1.409	20	1.391	10	0.5175	0.5193	11.21
1.345	30	1.312	5	0.5731	0.5739	127
1.302	10	1.308	5	0.5844	0.5837	218
					0.5856	00.30
		b=broad				

a_0=4.24 Å c_0=39.69 Z=3	a_0=4.15 Å c_0=39.19 Z=3	hexagonal cell
a_{rh}=13.45 Å α=18°08′ Z=1	a_{rh}=13.28 Å α=18°00′ Z=1	rhombohedral cell

1. Joseite A from Glacier Gulch, Hudson Bay Mountain, near Smithers, Omineca Mining Division, British Columbia[11].
2. Ikunolite from the Senju-maé vein, Kanagasé vein group, Ikuno mine, Hyogo Prefecture, Japan.

Cu/Ni radiation, λ=1.5418 Å ($2\theta<30°$), λ=1.5405 Å ($2\theta\geqq30°$).
Indices are based on hexagonal cell.

cell with $a_0=4.15$ Å and $c_0=39.19$ Å. These constants had been obtained by refining of those determined from the Weissenberg photographs about $[11\bar{2}0]$ axis on zero, first and second layers, and are close to those of joseite A[11]. Seeing from the appearance of the diffraction spectra with $h-k+l=3n$ and those of $h\bar{h}0l$ in which l is odd, the space group is determined as $R\bar{3}m$.

Crystal structure

The crystal structure of ikunolite was determined by single crystal method using the same cleavage piece as oscillated. That ikunolite has sheet structure similar to that of tetradymite [Bi_2Te_2S] is highly expectable from the presence of perfect basal cleavage[5]. Through the execution of trial and error method based on the probable positions of atoms given in International Table, they were assumed as $S_1=(0,0,0)$; $Bi_1=(0,0,x),(0,0,\bar{x})$; $Bi_2=(0,0,y),(0,0,\bar{y})$; and $S_2=(0,0,z),(0,0,\bar{z})$ in hexagonal co-ordination. Selenium is, as mentioned later, imterpreted as random substitute for sulphur in the ratio of S : Se=92 : 8. The intensities of basal reflections produced by rotation of the crystal about $[11\bar{2}0]$ axis were measured by diffractometer and converted into structure factors with reference to Lorenz factor, the correction of extinction effect being taken into consideration. In Table 4, the observed structure factors are compared with those which are calculated on the basis of the following parameters: $S_1=(0,0,0)$, $Bi_1=(0,0,0.142)$, $Bi_2=(0,0,0.287)$, $S_2=(0,0,0.426)$ (Fig. 3).

In the same way, the visually estimated intensities of the other reflections in the zero layer Weissenberg photograph are converted into structure factors, which are compared with calculated ones in Table 5. The reliability factor obtained from the numerical values in Tables 4 and 5 is 0.13.

The atomic distances given by the parameters are as follows:

$S_1-Bi_2=3.01$ Å, $S_2-Bi_2=3.01$ Å, $S_2-Bi_1=3.08$ Å, $Bi_1-Bi_1=3.10$ Å.

The smaller value between Bi_1 and Bi_1 which is nearly the same as

Table 4. Observed and calculated structure factors for $00l$ reflections.

hkl	F_{obs}	F_{calc}
003	12	−26
006	37	38
009	106	−118
00.12	128	−137
00.15	49	43
00.18	56	−56
00.21	268	268
00.24	31	9
00.27	43	38
00.30	65	−66
00.33	96	−115
00.36	28	−30
00.39	54	−53
00.42	133	188
00.45	18	28

Table 5. Observed and calculated structure factors for *hhl* reflections.

hkl	F_{obs}	F_{calc}
110	321	283
113	—	−23
116	45	40
119	85	−99
11.12	97	−117
11.15	—	37
11.18	—	−49
11.21	175	237
11.24	—	12
11.27	120	35
11.30	65	−62
11.33	116	−116
11.36	—	−29
11.39	59	−70
11.42	177	177
220	195	211

Bi-Bi distance in native bismuth probably means the covalent bonding.

The structure of ikunolite is summerized as follows:

Space group:	D^5_{3d}-R $\bar{3}$m.
Rhombohedral lattice:	$a_{rh}=13.28$ Å, $\alpha=18°00'$, $Z=1$.
Hexagonal lattice:	$a_0=4.15$ Å, $c_0=39.19$ Å, $Z=3$.
Parameters of atoms:	$S_1=(0,0,0)$, $Bi_1=(0,0,0.142)$,
	$Bi_2=(0,0,0.287)$, $S_2=(0,0,0.426)$.

The structure consists of hexagonally packed layers of sulphur (with random substitution by selenium in the ratio of S: Se=92: 8) and of bismuth, in the order S_1, Bi_2, S_2, Bi_1, Bi_1, S_2, Bi_2, S_1, Bi_2, S_2, Bi_1, Bi_1,···, and the perfect basal cleavage will be due to the weaker bond between bismuth and sulphur atoms than that between bismuth

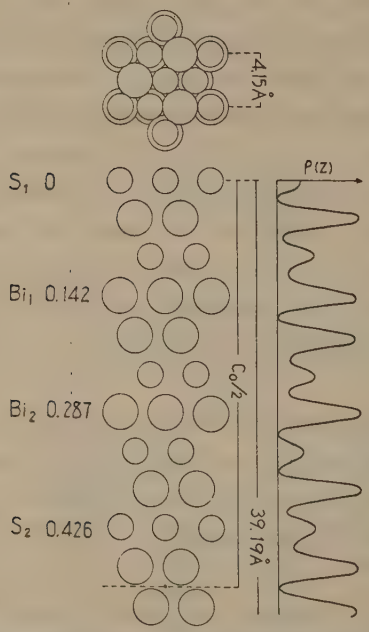

Fig. 3. Arrangement of atoms on $(10\bar{1}0)$ and Fourier synthesis of electron density along c-axis of ikunolite. The numbers denote the Z-parameters of atoms respectively.

and bismuth.

Figure 3 shows the arrangement of atoms with one dimentional Fourier projection of electron density along c-axis which depicts well the positions and effects of atoms.

Geochemical Consideration

The occurrences of selenium or tellurium minerals in xenothermal deposit have been reported from the Llallagua mine, Bolivia[12] (tetradymite associated with cassiterite) and the Suttsu mine, Japan[6] (the same assemblage as above). It is interesting that the tetradymites of Llallagua and Suttsu mines and the ikunolite of the Ikuno mine are the products of the earlier stage of mineralization in these xenothermal deposits, and that some minerals accompanying them are common in pneumatolytic or high temperature hydrothermal deposits. In this respect, it is worth mentioning that joseite in association with bismuthinite and tetradymite is reported to occur in quartz-feldspar vein of a tin deposit in Central Transbaikalia region[4].

The W-Bi-S-Se association in the Ikuno mine will correspond to the Sn-Bi-Te-S assemblage from Llallagua, Suttsu and Central Transbaikalia region.

The Se : S ratio in pneumatolytic and high temperature hydrothermal sulphides as high as 1 : 400 which was reported by Goldschmidt and Strock[3] suggests the possible occurrence of such selenium-bearing minerals as ikunolite as the product of higher temperature mineralization.

Diadochy between sulphur and selenium

The diadochy between sulphur and selenium is observed in the following minerals in which bismuth minerals are prevailing (Table 6). So, the diadochic substisution of sulphur and selenium probably takes place in ikunolite as well.

Table 6. Minerals with S-Se diadochy.

Minerals	Cryst. system	Chem. comp.	Ref.
Bismuthinite	Orthorhombic	Bi_2 (S, Se)$_3$	9)
Guanajuatite	Orthorhombic	Bi_2 (Se, S)$_3$	9)
Paraguanajuatite	Rhombohedral	Bi_2 (Se, S)$_3$	10)
Csiklovaite	Rhombohedral	Bi_2Te (S, Se)$_2$	8)
Tetradymite	Rhombohedral	Bi_2Te_2 (S, Se)	9)
Cadmoselite	Hexagonal	Cd (Se, S)	1)
Galena-Clausthalite	Cubic	PbS-PbSe	2)
Metacinnabar	Cubic	Hg (S, Se)	9)

Acknowledgements

The writer wishes to express his sincere thanks to Professor Takeo Watanabe for his guidance, to Dr. Yoshio Takéuchi and Dr. Yoichi Iitaka of University of Tokyo for their helpful suggestions concerning structure analysis of the mineral and to Dr. Takashi Katsura of Tokyo Institute of Technology for his courtesy in chemical analysis of the mineral. Also hearty thanks of the writer are subjected to Messrs. Rokuzo Shirai and Kuniharu Horikawa, Geological Section of the Ikuno mine, for their kind assistance in the field survey and presentation of the specimen.

References

1) Bur'yanova, E. Z., G. A. Kovalev and A. L. Komkov: Zap. Vses. Mineralog. Obshch., **86**, 626-628 (1957) (in Russian).
2) Coleman, R. G.: Amer. Miner., **44**, 166-175 (1959).
3) Goldschmidt, V. M. und L. W. Strock: Nachr. Ges. Wiss. Göttingen, Math.-physik. Klasse IV, N. F. 1, No. 11, 123 (1935).
4) Grigoriev, I. F. and E. I. Dolomanova: Trudy Mineral. Muz. Akad. Nauk S. S. S. R., 7, 154-157 (1955) (in Russian) (Miner. Abst., **13**, 160 (1957)).
5) Harker, D.: Zeit. Krist., **89**, 175-181 (1934).
6) Ishibashi, M.: Jour. Fac. Sci. Hokkaido Univ. VIII-2, 97-106 (1952).
7) Kato, T.: Jap. Jour. of Geol. and Geogr., **5**, 126-133 (1928).

8) Kock, S.: Acta Miner. Petr., Publ. Miner. Petr. Inst. Univ. Szeged., **2**, 1-23 (1948) (Miner. Abst., **10**, 509 (1948)).
9) Palache, C., H. Berman and C. Frondel: The System of Mineralogy, 7th Ed. vol. 1 (1944).
10) Ramdohr, P.: Com. Rec. Min. Mex., **20**, 1 (1948).
11) Thompson, R. M.: Amer. Miner., **34**, 342-382 (1949).
12) Turneaure, F. S.: Econ. Geol., **30**, 14-60, 170-190 (1935).

Manuscript received June 6, 1959.

Mineralogical Journal, Vol. 2, No. 6, pp. 408-421, Aug., 1959

THE MINERALS OF THE NODA-TAMAGAWA MINE, IWATÉ PREFECTURE, JAPAN

I. Notes on Geology and Parageneses of Minerals

Takeo Watanabe

Geological Institute, University of Tokyo

Abstract

The ore deposits of the Noda-Tamagawa mine have become famous for their wealth of mineral species, the production of high grade manganese ores, and also the recent discovery of uranium ores. More than seventy minerals have been found in this mining area including such rare minerals as pyrochroite, manganosite, vredenburgite, yoshimuraite (a new mineral of Ba, Sr, Mn, Ti-silicate), etc.

The ore deposits of this mine may be classified into the following types:

(A) The contact-metamorphosed bedded manganese deposits in metamorphosed roof pendant in the batholithic mass of granitic rocks.

(B) (1) The uranium-bearing veins.
(2) The cobalt-nickel-molybdenum-bearing uranium deposits associated with pelitic hornfels.

(C) Pyrometasomatic copper-bearing pyrrhotite deposits found in limestone.

(D) Gold-silver-bearing quartz-arsenopyrite veins.

Among them manganese deposits are economically the most important ones. The geology and ore deposits of the mine are briefly described. The mineral parageneses of ores and country rocks are shown in Tables 1 and 2.

Introduction

The Noda-Tamagawa mine, one of the important manganese producers in Japan, is located about 16 km. south-east of Kuji City, in the north-eastern part of Iwaté Prefecture (Fig. 1).

The mine had been almost unknown before the discovery of a rich primary manganese ore-body below the oxidized zone in 1948. Not far from this manganese ore zone lies the copper-bearing pyr-

rhotite deposit which was once exploited for copper in 1919. In order to know the genetic relation between the manganese deposits and the cupriferous pyrrhotite deposits the author, together with his student Mr. S. Yui, began to study the geology of this mining district. In the course of his study the author discovered abundant occurrences of manganese minerals which have hitherto been known as rare minerals. More than fifty thousand tons of the pyrochroite-manganosite ore has been shipped to the smelter for metallurgical uses. Various kinds of manganese silicate minerals have also been found. The paragenesis of minerals of the deposits is very complex and resembles in some degrees those of Kaso, Långban and Franklin.

Furthermore, the new occurrence of uranium minerals has recently been recorded.

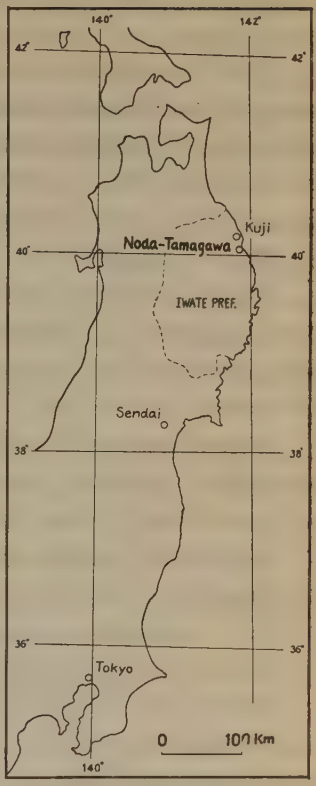

Fig. 1. Index map showing the location of the Noda-Tamagawa Mine.

In this paper the author wishes to present a brief explanation of the occurrences of minerals, geologic setting, and his hypothesis of the origin of the deposits.

Detailed description of the minerals of this remarkable mining district will be given in future papers.

Previous Works

The Noda-Tamagawa mine had not been known as a mineral locality before K. Kawai[3] reported in 1933 the occurrence of

penwithite, a neotocite-like mineral, associated with manganese ores of this mine.

Later the mine was visited by T. Yoshimura[17] and he found some interesting manganese minerals among which picrourbanite and riebeckrichterite were discovered and described in 1937. The optical properties and chemical composition of these minerals were given in his book "The manganese deposits of Japan"[18] published in 1952.

In the course of his geochemical study of the manganese deposits of Japan, J. Kitahara[4][5] studied the manganese deposits and later recorded the occurrence of the crystals of arsenopyrite from the quartz vein in 1940.

A brief description of the geology of the Noda-Tamagawa manganese mine was given by M. Doi[1] just after the discovery of the rich part of the Misago ore body in 1949.

In 1951 the author and S. Yui began to study the geology and ore deposits of the Noda-Tamagawa mine, and the next year, the outline of geology and mineral paragenesis are described by Yui in his graduation thesis presented to the University of Tokyo.

Genesis and contact-metamorphism of the manganese deposits were discussed by the author[15] in 1953. He concluded that the deposits were originally of exhalative-sedimentary type and later contact-metamorphosed due to the granitic intrusion.

In his comprehensive work on manganese minerals of Japan D. E. Lee[6] recorded the occurrence of hausmannite, pyrophanite, picrotephroite, rhodonite, neotocite, bementite, etc. in the Noda-Tamagawa mine. The result of a chemical analysis of the picrotephroite is given in this paper.

In 1952 H. Miyamoto[7], Y. Ishida and other members of the Geological Survey of Japan carried out geological and geochemical survey of this mining area and published their paper.

During the extensive prospecting for uranium ores in the Kitakami Mountain district, a new occurrence of uranium-bearing ores

was announced by Y. Okumi[8] et al., geologists of the Geological Survey of Japan, in 1957. Since then, detailed underground survey has been carried out by geologists of the mine and the Geological Survey of Japan. The paragenesis of uranium ores was first described by T. Hamaji[2] and Y. Sakamaki, geologists of the Geological Survey of Japan, in 1957.

T. Takeuchi[12] and M. Nambu engaged in microscopic investigation of copper-bearing pyrrhotite ore of the Shinmaida ore body and they found cubanite in 1953. This deposit was again surveyed by A. Sugaki[11] and H. Abe in 1957. An analysis of hausmannite in the rich manganese ore was given by K. Omori[9] and S. Hasegawa in 1955.

An excellent geologic account of the Noda-Tamagawa manganese deposits was given by A. Sato[10], K. Fukuda and T. Wada, geologists of the Shinkohatsu Mining Company in 1957.

Since 1951 the author has frequently visited the mine and there have been many additions to the list of minerals of Noda-Tamagawa.

Outline of Geology and Ore Deposits

(*a*) *Geology*

The rocks in the mining district consist mainly of slate, sandstone, thin-bedded chert, massive chert and limestone of unknown age. Lithologically, they resemble the rocks of the Palaeozoic (Chichibu) formation extensively developed in the northern part of the Kitakami Mountainland. These rocks have been strongly folded and compressed, and they have been intruded and thermally metamorphosed by the granitic magmas of probable Cretaceous age. Therefore, the rocks may be described as slaty hornfels, arenaceous hornfels, thin-bedded meta-chert, massive quartzite and crystalline limestone.

In the northeastern part of the district, these older rocks are covered unconformably by the upper Cretaceous beds belonging to

the Kuji formation and the Tertiary beds of the Noda formation. Moreover, the Quaternary terrace deposits cover extensively all the formations above mentioned.

Due to the severe deformation the older formation stands in steeply inclined beds and is tightly folded in many places. The prevailing strike is northwest, but N. 10°~20° W. in the eastern

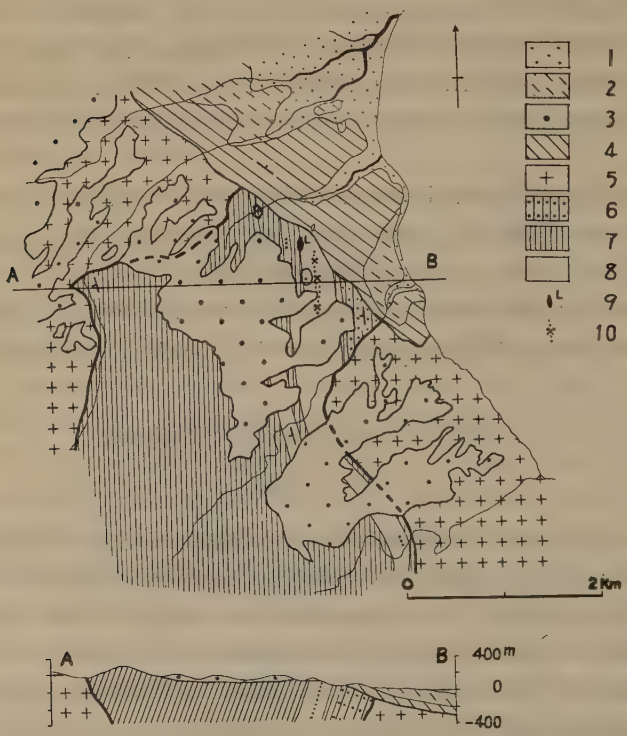

Fig. 2. Geological map and section of the Noda-Tamagawa mining area. (After Yui and Fukuda)

1. Alluvial formation. 2. Lower terrace deposits. 3. Higher terrace deposits. 4. Kuji Mesozoic formation. 5. Akka granite (granodiorite). 6. Sandstone-hornfels. 7. Pelitic hornfels. 8. Siliceous hornfels of chert origin. 9. Limestone (Shinmaida copper-bearing pyrrhotite deposit of pyrometasomatic type). 10. Manganese ore zone.

part. The dip is generally 60°~85° west.

The country rocks of the manganese deposits consist of highly thermal-metamorphosed meta-cherts including massive and thin-bedded quartzite and biotite hornfels. They strike generally N. 10° ~20° E. and dip nearly vertically. Generally the structure is very simple but locally it is very complex, the country rocks together with ore bodies having been strongly folded into sharp syncline or anticline plunging about 45° to the southwest. The linear structure, due to the crinkle of the rocks and minor foldings, is generally parallel to the major fold axis. The geological sketch map is shown in Fig. 2.

(*b*) *Ore deposits*

The ore deposits of the Noda-Tamagawa mine may be classified tentatively into the following types:

(A) Manganese deposits.
(B) Uranium deposits.
  (1) Vein type.
  (2) Hornfels type.
(C) Copper-bearing pyrrhotite deposit of pyrometasomatic type.
(D) Gold-silver-bearing arsenopyrite-quartz-carbonate veins.

Economically the manganese deposits are the most important.

(A) *Manganese deposits*

The manganese deposits in the mining area are found exclusively in meta-cherts. They are of bedded type and have been thermally metamorphosed into complex ores. Three ore zones have hitherto been known and named respectively, the Shinmaida, Misago and Kamishiro ore zones among which the second is the most productive and important.

The distribution of chert suggests that the Maida, Takada, Misago and Kirihata ore bodies are at essentially the same stratigraphic horizon called the Misago ore-zone. This zone can be traced about 1,200 m. along the strike on the surface and is known

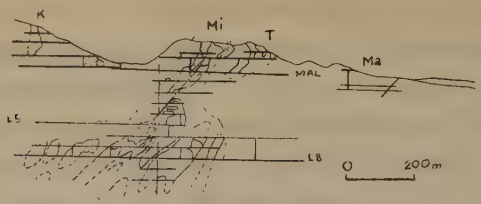

Fig. 3. Longitudinal section of the Misago manganese ore zone of the Noda-Tamagawa mine.
K: Kirihata, Mi: Misago, T: Takada and Ma: Maida ore bodies.

to be more than 300 m. in depth. The manganese ores form lenticular beds between thin-bedded meta-chert and massive quartzite. The ore bodies range in length from one meter to two hundred meters along the strike and are usually elongated along the lineation of the country rocks or along the plunging axis of the folds. The ratio of the longest diameter of each ore body to the shortest along the bedding plane is more than three. Thickness of the mined ore bodies ranges from a half to three meters.

The manganese ores in this mine may be roughly divided into the following types according to their mineral content:

(1) Pyrochroite ore (Kimiman- or Kibiman-kô).
(2) Manganese carbonate ore (Tanman-kô).
(3) Hausmannite ore (Tetsuman-kô).
(4) Braunite ore.
(5) Tephroite ore (Tefuro-kô).
(6) Rhodonite ore (Bara-kô).
(7) Alabandine ore (Ryûman-kô).
(8) Low grade ore of manganiferous hornfels type.
(9) Supergene manganese oxides ore (Ni-sanka mangan-kô).

The grade of these ores and their important constituent minerals are shown in Table 1. It is very interesting to note that pyrochroite, manganosite and other manganese silicates hitherto known as very rare are very common in this mine and occur abundantly as important ore minerals.

anese ores of the Noda-Tamagawa deposits and their important constituent minerals.

ganese-nate ore	Hausmannite ore	Braunite ore	Tephroite ore	Rhodonite ore	Alabandine ore	Manganiferous hornfels ore	Supergene manganese oxide ore
ıman)	(Tetsuman)		(Tefuro)	(Bara)	(Ryûman)		(Ni-sanka)
~50	50~60	50~55	44~50, 38~44	26~32, 20~25	44~54	10~20	80~85 (MnO_2)
~1.5	1~2	2~5	5~10	3~5	1~5		
~7	3	15~20	25~30	30~40	10~15	40~60	5
+	++	—	—	—	—	—	—
+	+	—	+	—	—	—	—
+	+	—	+	—	—	—	—
+	+++	++	+	—	—	—	—
—	++	+	—	—	—	—	—
+	+	+	+	+	+	+	—
+	+	+	+	—	+	—	—
+	+	+	+	+	+	+	—
—	+	+++	+	+	+	+	—
++	++	++	+++	+	++	+	—
+	+	+	++	+	+	+	—
—	—	+	+	++	++	+	—
—	—	+	++	+++	++	++	—
—	—	+	++	++	+	++	—
—	—	—	+	+	—	+	—
—	—	+	+	+	—	++	—
—	—	+	+	+	+	++	—
+	++	+	+	+	—	++	—
+	+	—	+	—	+	+	—
+	+	+	+	+	+	+	—
+	+	+	+	++	+	+	—
++	++	+	++	++	++	+	—
+	—	+	+	+	+++	+	—
+	+	+	+	+	+	+	+
—	—	—	—	—	—	—	+++
—	—	—	—	—	—	—	+++
—	—	—	—	—	—	—	+
—	—	+	+	+	+	+	+
—	—	+	—	+	—	+	++

+ abundant.

Table 1. Types of mang

	Kind of ore	Pyrochroite ore	Man carbo
	(Local name)	(Kibiman or Kimiman)	(T
	Mn %	50～58	4
	Fe %	0.5	0.
	SiO_2 % / Mn %	5	
Manganosite	77.4	++	
Pyrochroite	62	+++	
Hydrohausmannite	63	++	
Hausmannite	72	+	
Vredenburgite	50～60	—	
Jacobsite	23.8	—	
Galaxite	20	+	
Pyrophanite	36	+	
Braunite	63.6	—	
Tephroite	54.5	++	
Alleghanyite	56	+	
Spessartine	33	—	
Rhodonite	40	—	
Pyroxmangite	42	—	
Bustamite	35	—	
Urbanite	5～8	—	
Richterite	10	—	
Manganophyllite	4～15	+	
Manganphlogopite		++	
Bementite	39	+	
Neotocite (Penwithite)	10～27	+	
Rhodochrosite	47.8	+++	+
Alabandine	63.2	+	
Baryte	0	+	
Pyrolusite	63.2	—	
Cryptomelane (Ramsdellite)	63	—	
Psilomelane	63	—	
Feldspar	0	—	
Quartz	0	—	

— none, + rare, ++ common, ++

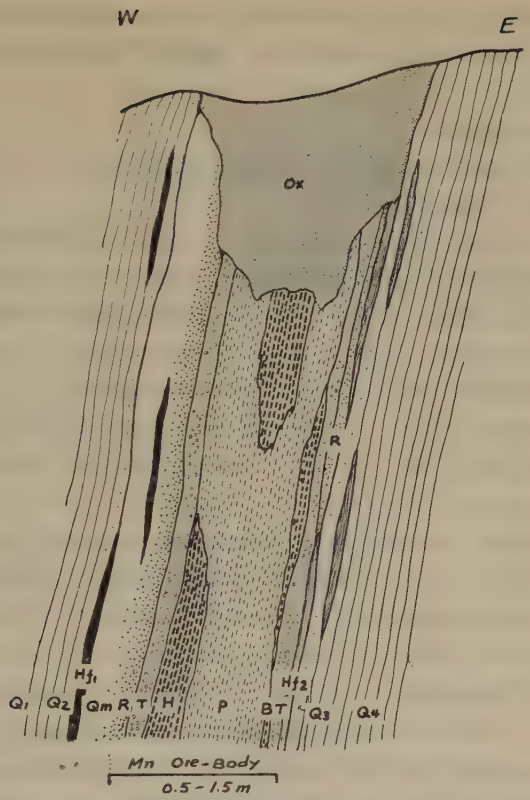

Fig. 4. Idealized cross section of the manganese ore zone of the Noda-Tamagawa mine, showing the bedded arrangement of manganese ores and country rocks. Vertical length of this section is diminished.

Ox: Oxidized zone consisting mainly of manganese dioxide ores.
Hf_1: Pelitic hornfels of the hanging wall (often uraniferous).
Hf_2: Pelitic hornfels of the foot wall (manganiferous).
Q_1: Thin-bedded meta-chert of the hanging wall.
Q_2: Thin-bedded meta-chert of the hanging wall in the manganese ore zone.
Q_3: Thin-bedded meta-chert of the foot wall in the manganese ore zone.
Q_4: Thin-bedded meta-chert of the foot wall.
Q_m: Massive meta-chert containing small amounts of manganese minerals.
R: Rhodonite zone. T: Tephroite zone. H: Hausmannite ore. P: Pyrochroite-manganosite ore zone.

Petrographically most of these ores show very fine banding structure. They occur usually in regular band in ore zones as shown in Fig. 4.

(B) *Uranium deposits*

Uranium deposits may be classified into the following two types: (1) vein and (2) hornfels types.

(1) Vein type: Uranium occurs in molybdenite-bearing quartz veins cutting the bedded manganese deposits along faults or joints. Although the width of the veins is usually narrow, comparatively high grade ores (0.5% U) occur in localized parts of the veins. The reserve of uranium ores of this type is not large.

(2) Hornfels type: As shown in Fig. 4 uraniferous pelitic hornfels of lenticular form occurs always on the hanging wallside and is often associated with massive meta-chert.

The hornfels rich in uranium is macroscopically very dark due to higher content of carbonaceous matter and sulphides. Some uraniferous hornfelses contain as much as 0.15% U. Constant association of nickel, cobalt, vanadium, molybdenum with the uranium-bearing hornfels has been detected by fluorescent X-ray method. The characteristic occurrence and stratigraphic localization of the uranium ores suggest that the uranium was precipitated syngenetically together with iron, nickel, cobalt, molybdenum, etc.

(C) *Copper-bearing pyrrhotite deposit of pyrometasomatic type*

A copper-bearing pyrometasomatic pyrrhotite deposit occurs in the limestone area of the Noda-Tamagawa concession and has been known as the Shinmaida deposit since about 1920. The pyrrhotite ores are included in lenticular blocks of saccharoidal limestone as shown in the geological map (Fig. 2). The principal minerals are garnet, sahlite, calcite, pyrrhotite and sphalerite. The ore contains 0.5~1% of copper in the form of chalcopyrite and 15~38% of iron mainly in the form of pyrrhotite.

(D) *Gold-silver-bearing arsenopyrite-quartz-carbonate veins*

In the course of the prospecting of the manganese deposits of

the Misago ore zone, narrow veins contaning gold, silver and arsenopyrite were discovered. They occur along the strike faults in meta-cherts near the manganese ore-bodies.

Parageneses of the minerals

As the genetic history of the ores and rocks of the Noda-Tamagawa mining area is not so simple, the parageneses of minerals are very complex as well. The minerals hitherto found in this mining area, may be genetically classified into the following groups:

(1) Recrystallization products due to the thermal metamorphism.
  (a) Minerals in manganese ores.
  (b) Minerals in hornfelses.
(2) Pyrometasomatic products.
  (a) Minerals in manganese ores.
  (b) Minerals in limestone or "skarn".
(3) Pegmatitic or pneumatolytic products in or near the manganese ores.
(4) Hydrothermal products.
  (a) Minerals replacing manganese ores.
  (b) Minerals of the veins cutting manganese ores.
  (c) Minerals of the gold-silver-bearing quartz-carbonate veins cutting hornfels.
(5) Supergene oxidation products.
  (a) Minerals found in the oxidized zone of manganese deposits.
  (b) Minerals found in the oxidized zone of copper-bearing pyrrhotite deposits.

In Table 2 the minerals have been arranged according to the above-mentioned classification.

(1) *Recrystallization products*

As will be discussed later, most of the minerals constituting the manganese deposits may be recrystallization products from the syngenetic manganese carbonate and oxide ores due to thermal

metamorphism of granite intrusions. Among many manganese minerals pyrochroite after manganosite, hausmannite, braunite, tephroite, rhodonite and rhodochrosite, make up nearly the whole mass of the manganese ores. The manganese ores which are considered to be recrystallization products show the characteristic mozaic texture under the microscope. Biotite, cordierite and andalusite are commonly found in pelitic hornfelses.

(2) *Pyrometasomatic products*

Pyrometasomatic products may be divided into two groups, manganese skarn and lime-silicate skarn.

Pyrometasomatic manganese skarn occurs along the contact between pegmatitic mass and manganese ore bodies. Rich manganese carbonate ores are often zonally bordered by massive tephroite and rhodonite.

Pyrometasomatic lime-silicate skarn occurs in limestone at Shinmaida and consists essentially of garnet, sahlite associated with pyrrhotite, chalcopyrite and sphalerite, etc.

The formation of these skarns may be attributed to metasomatic action of pegmatitic solutions derived from the later granitic magmas.

(3) *Pegmatitic products near the manganese deposits*

Peculiar pegmatitic rocks consisting mainly of barium-bearing feldspar, rhodonite, urbanite and richterite are often found on the foot-wall side of the Misago ore zone immediately adjacent to the manganese ores. Recently a new mineral, yoshimuraite, has been discovered by the author in this rock. Judging from the peculiar mineral association an intense interaction between manganese ores and pegmatitic solutions derived from the granitic magma might have taken place during the crystallization of the pegmatitic solutions. This peculiar pegmatitic facies may well correspond to the alkali facies of granite at granite-dolomite contacts in Skye described by C. E. Tilley[14] in 1949.

(4) *Hydrothermal products*

Along faults and joints occur various kinds of hydrothermal veins which were probably formed during the later stage of granitic intrusion. The hydrothermal veins which cut the manganese deposits are rich in such manganese minerals as rhodonite, bementite, neotocite, mangancalcite, etc., while veins cutting siliceous rocks consist mainly of quartz.

Influence of chemical nature of the wall rocks to the vein stuff is very remarkable.

(5) *Supergene oxidation products*

Black manganese oxide ores were mined during the earlier stage of the exploitation of this mine. Most of supergene manganese ores have been exhausted. However, the occurrences of psilomelane and ramsdellite have been known in this mine.

Several supergene copper and iron minerals have also been discovered as shown in Table 2.

Origin of ores

As seen from the complex mineral parageneses of various kinds of rocks and ores of the Noda-Tamagawa mine, their origin may not be simple. Previous investigators like Yoshimura[18] and Kitahara[4] offered metasomatic-emplacement hypothesis. They considered that main ore-bodies were formed by metasomatic emplacement due to hydrothermal action in the cherty rocks before the intrusion of the granitic rocks. However, Lee[6] suggested the theory of high temperature hydrothermal replacement of selected chert in connection with granitic intrusion according to his study of the mineral paragenesis of ores in laboratory.

The manganese deposits found in the Chichibu Terrain in Japan are always bedded with rhythmic or massive cherts or meta-cherts. In less metamorphosed area the fine rhythmic sedimentary banding of constituent minerals is well observed. Manganese carbonate and oxide ores are often associated with radiolarian chert. The similar

occurrence of manganese ore beds was described by N. L. Taliaferro[13] in 1943.

The similar field relations between manganese ores and metacherts are also observed in the Noda-Tamagawa mining areas as explained before. But primary sedimentary textures of the manganese ores have sometimes been obliterated by later thermal metamorphism and also by invasion of pegmatitic and hydrothermal solutions derived from the later granitic magmas.

Taking all the field data and laboratory observations into consideration, it is concluded that the manganese ores were originally chemical sediments deposited syngenetically with the enclosing cherts and subsequently were metamorphosed.

As to the source of manganese and silica forming ores and cherty sediments, it is believed that both of them were probably derived from the same source such as submarine hot springs in geosynclinal basin. Therefore, the main part of the Noda-Tamagawa manganese deposits should be classed into the thermally metamorphosed exhalative sedimentary types.

According to the author's opinion uraniferous hornfelses were also originally chemical sediments containing the carbonaceous matter, nickel, cobalt, molybdenum, etc.

The Shinmaida copper-bearing pyrrhotite deposits may, however, belong to the ordinary pyrometasomatic type.

Acknowledgements

The author is grateful to President Y. Yokobori and other members of the staff of the Shinkohatsu Mining Company. Special thanks are due to Mr. K. Saida, General Manager, and T. Wada, A. Sato and K. Fukuda, mining geologists of the Company for the valuable information and for the aids during his field work. Thanks also are due to Mr. S. Yui, Dr. A. Kato, and Miss Den for their help during the preparation of this paper.

The investigation was aided by a grant from the Scientific Research Fund of the Ministry of the Education.

References

1) Doi, M.: Special publication of the Japan Mining Industry Assoc., Ser. No. 1, 34 (1949) (in Japanese).
2) Hamaji, T. and Y. Sakamaki: Mining Geol., 7 (4), 313 (1957) (in Japanese).
3) Kawai, K.: Jour. Geol. Soc. Jap., 40, 348 (1933) (in Japanese).
4) Kitahara, J.: Jour. Geol. Soc. Jap. 57, 338 (1951) (in Japanese).
5) ———: Jour. Geol. Soc. Jap. 58, 545 (1952) (in Japanese).
6) Lee, D. E.: Stanford Univ. Publ. Univ. Ser. Geol. Sci., 5, 1 (1955).
7) Miyamoto, H. and Y. Ishida: Bull. Geol. Surv. Japan, 8 (2), 13 (1957) (in Japanese).
8) Okumi, Y., T. Hamaji, J. Okano and Y. Sakamaki: Rept. Symposium for Atom. Energ., No. 2, B-63, 131 (1958) (in Japanese).
9) Omori, K. and S. Hasegawa: Jour. Jap. Assoc. Miner. Petrol. Econ. Geol., 41, 171 (1957) (in Japanese).
10) Sato, A., K. Fukuda and T. Wada: Mining Geol., 7 (23), 13; 7 (24), 98 (1957) (in Japanese).
11) Sugaki, A. and H. Abe: Unutilized iron resources of Japan in 1956 No. 3, 223 (1957) (in Japanese).
12) Takeuchi, T. and M. Nambu: Bull. Res. Inst. Mineral Dress. & Metall. 9, (1953) (in Japanese).
13) Taliaferro, N. L.: Calif. Div. Mines Bull. 125, 277 (1943).
14) Tilley, C. E.: Geol. Mag., 86, 7 (1949).
15) Watanabe, T.: Jour. Geol. Soc. Japan, 58, 336 (1952) (in Japanese).
16) ———: Mining Geol., 7, 87 (1957) (in Japanese).
17) Yoshimura, T.: Jour. Geol. Soc. Japan, 44, 561 (1937) (in Japanese).
18) ———: Manganese deposits of Japan, (1952) (in Japanese).

Manuscript received July 1, 1959.

Mineralogical Journal, Vol. 2, No. 6, pp. 422-426, Aug., 1959

SHORT COMMUNICATIONS

MELILITE CRYSTAL IN THE CAVITY OF BLAST-FURNACE SLAG

Hideo Minato

Institute of Earth Science, College of General Education, University of Tokyo

When the writer visited the Yawata Iron Works in the year before last, he found small idiomorphic crystals of melilite in cavities of blast-furnace slag which had been left in a ballastyard.

Description of the crystal. The crystal in cavities is as large as $0.4 \times 0.4 \times 1$ mm., and stout prismatic, consisting of a tetragonal prism and the base (Fig. 1)*. Colourless and transparent, with vitreous lustre. Cleavage: (100) distinct and (001) indistinct. Hardness: 5.5.

The slag has a porphyritic texture with phenocrysts of melilite, which displays a characteristic zonal structure under the microscope as illustrated in Fig. 2B. The optical property of the melilite implies that its nucleus (B_1 in Fig. 2B) is highest in the content of gehlenite molecule, while the rim (B_3 in Fig. 2B) is lowest.

Although zonal structure is not so distinct in the melilite crystal from cavities, a thin layer with higher content of gehlenite molecule (A_1 in Fig. 2A) prevails along the border of groundmass, and another layer with lower content of gehlenite molecule (A_3 in Fig. 2A) covers the top of the crystal.

Materials for chemical analyses. Sample A, the pure material of

* Two good crystals were measured with a V. Goldschmidt's two circle goniometer, but no pyramidal face was observed.

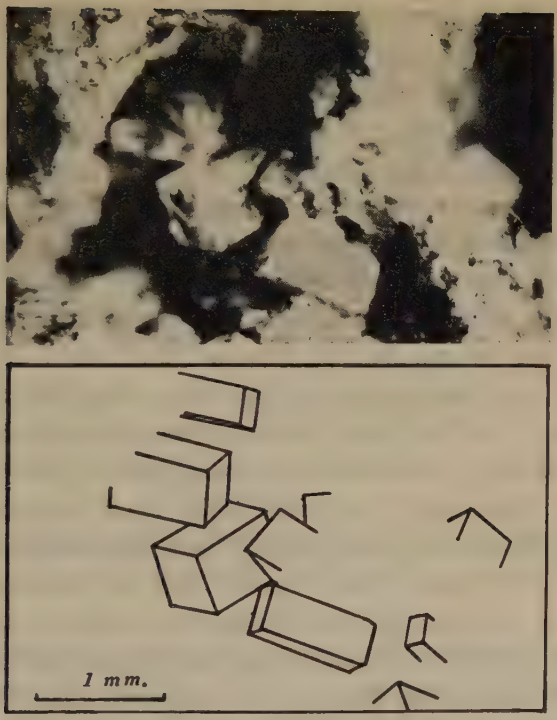

Fig. 1. Melilite crystal in a cavity of blast-furnace slag from Yawata Iron Works.

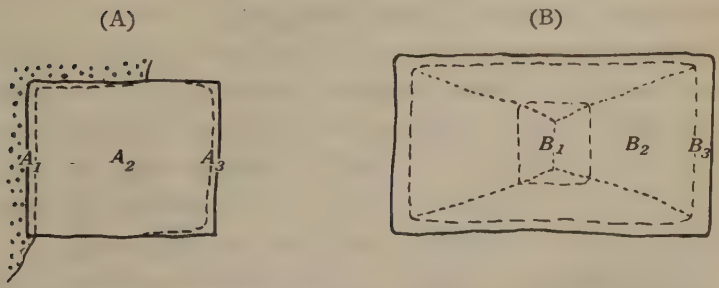

Fig. 2A. Zonal structure of melilite crystal under the microscope. (Idiomorphic crystal in the druse of slag)

Fig. 2B. Zonal structure of melilite under the microscope. (Melilite phenocryst in the massive part of slag)

the melilite in cavities, was easily obtained by hand-picking under the binocular microscope.

Sample B which is mainly composed of clear part of the melilite phenocryst corresponding to B_2 in Fig. 2B was obtained from 200~250 mesh fraction of powdered slag by using magnetic separator, isodynamic separator, heavy liquid and binocular microscope.

Both A and B samples had been examined under the polarizing microscope before they were analysed.

Procedure of chemical analysis. Each sample was divided into two lots, one for the determination of SiO_2 content and the other for $H_2O(-)$, ignition loss, Al_2O_3, TiO_2, Fe_2O_3, MgO and CaO.

One lot of 6~7 mg. was fused with sodium hydroxide and silica was determined by colorimetry with molybdenum blue[2)3)].

Of the other lot of 6~7 mg., $H_2O(-)$ and ignition loss was measured first, then it was treated with hydrofluoric acid and sulfuric acid to eliminate silica. The residue was dissolved in dilute hydrochloric acid, and iron, aluminium and titanium were precipitated with ammonium chloride and ammonium hydroxide. The filtrated precipitate was ignited and weighed, then titanium and ferric iron were determined colorimetrically, alumina being given by difference. Calcium was isolated as calcium oxalate and titrated with potassium permanganate solution, while magnesium was isolated with oxine salt and weighed as magnesia.

Chemical composition. Table 1 shows the results of chemical analyses and atomic ratios calculated on the basis of O=7, ignition loss and $H_2O(-)$ being neglected. The chemical composition of the melilites, both A and B, is in good accordance with the formula $Ca_2(Mg, Fe, Ti, Al, Si)_3O_7$[1)4)]. The molecular ratio of gehlenite to åkermanite is 68 : 32 for A and 55 : 45 for B respectively.

X-ray examination. About 15 mg. of each material was packed in a specially designed sample holder and its X-ray powder lines were measured by using "Norelco" X-ray spectrometer. The main powder lines of each material correspond to the composition ob-

Table 1. Chemical composition of melilites in blast-furnace slag.

(A) Melilite crystal in cavity					(B) Melilite in massive part				
Wt.%		Mol. prop.	Atom. rat.		Wt.%		Mol. prop.	Atom. rat.	
SiO_2	28.25%	,474	Si 1.31		SiO_2	29.05%	,484	Si 1.35	
TiO_2	1.23	,015	Ti 0.04		TiO_2	0.53	,006	Ti 0.02	
Al_2O_3	23.47	,228	Al 1.26	2.98	Al_2O_3	20.87	,203	Al 1.13	3.03
Fe_2O_3	1.97	,012	Fe 0.07		Fe_2O_3	2.00	,013	Fe 0.07	
MgO	4.45	,110	Mg 0.30		MgO	6.64	,164	Mg 0.46	
CaO	40.58	,723	Ca 2.00		CaO	40.20	,717	Ca 2.00	
Ig. loss	0.84		O 7.00		Ig. loss	0.98		O 7.00	
$H_2O(-)$	non.				$H_2O(-)$	non.			
Total	100.79%				Total	100.27%			

Analysed by H. Minato in 1959.

tained by chemical analysis, while some doublets and triplets infer the presence of zonal structure which is observed under the microscope as well.

Crystallization of melilite in cavities. The composition of the melilite crystal in cavities of blast-furnace slag is higher in gehlenite content than the melilite phenocryst from the neighbouring massive part, while the zonal structure of the latter indicates the crystallization course from gehlenite rich to åkermanite rich melilite, which is reasonable in those range of melilite series from the viewpoint of phase diagram. So, the melilite in cavities cannot be the product of later stage or fractional crystallization of the slag. Possibly, the gas, which had been released from cooling slag to form bubbles played an important role in mineralization in cavities.

Acknowledgements. The writer wishes to express his sincere thanks to Prof. Nobuo Katayama, University of Tokyo, and Mr. Yuichi Nishitomi, Yawata Chemical Industry Co. Ltd., for their kind helps during this investigation. He is indebted to Miss Nobuko Yoshii and Mr. Akira Kawahara for their assistance in the chemical analyses. He is very greatful to Dr. K. Wada, Super-

intendent of Technical Research Institute of Yawata Iron and Steel Co. Ltd., and Dr. T. Yoshida, Superintendent of Tobata Works of Yawata Chemical Industry Co. Ltd., to whom he owed the specimens used in this study.

References

1) Berman, H.: Amer. Mineral., **14**, 389 (1929).
2) Boltz, D. F.: Colorimetric Determination of Nonmetals, New York (1958).
3) Minato, H. and T. Kato.: Jour. Ceram. Ass. Japan, **66**, 141 (1958). (in Japanese)
4) Smith, J. V.: Amer. Mineral., **38**, 643 (1953).

Manuscript received July 10, 1959.

ABSTRACT OF THE KOBUTSUGAKU ZASSHI,

JOURNAL OF THE MINERALOGICAL SOCIETY
OF JAPAN, VOL. 4, NOS. 1-2,
January, 1959

Address

On the Theory of Twinned Space Groups (pp. 1-14)

Ryoichi Sadanaga

The theory of twinned space groups and its application to the structure determination of crystals, both developed by T. Ito and his collaborators, have been reviewed with special reference to the theory of groupoid and the Fourier-transform method for interpretation of X-ray diffraction patterns.

It is a well-established fact that polysynthetic twinning occurs in crystals on the scale of their unit cells. As the result of this mode of twinnining, some of the sets of symmetry elements in the structure cease, under certain conditions, to be effective throughout the crystal space, but are rendered valid only within a limited domain in the space. We call symmetry elements in these sets local symmetry elements. Thus, when we study the symmetry and the structure of a polysynthetically twinned crystal, we are to deal with the combination of sets of local symmetry elements with those of ordinary elements, and the mathematical theory for the combination of this kind is known as the groupoid theory.

X-ray diffraction patterns of these polysynthetic crystals are characterized by the appearence of extra rules of extinction and by the enhancement of symmetry in intensity distribution among special sets of reflections. These facts are given a simple interpretation in terms of the local symmetry elements in the structure with the aid of the Fourier-transform method.

Finally, emphasis is placed upon the fact that the presence of local

symmetry elements in the structure is also related to the occurrence of pseudo-symmetry in the outward form of the crystal, and the possibilities of future development of the study on polysynthetic structures are discussed.

Original Articles

Cause of Colouring of Anhydrite (*Part II*) (pp. 15-23)

Kenji Togari

In conection with the results of previous works, quantitative measurements were carried out to clarify the cause of colouring of anhydrite. The curve of absorption intensity versus frequency of light wave were obtained for pale blue and pale pink anhydrites from Yonaihata at every 50°C. from room temperature to 400°C., at which they become colourless. Summary of the results is illustrated in Figs. 3 and 4, both of which depict two absorption peaks, a sharp one in ultraviolet range and a broad one in visible range. The wave length of the latter peak of the pale blue variety is longer than that of pale pink one, and its intensity of each variety gradually diminishes as temperature rises. These results imply that the colouring of anhydrite is due to the presence of colour-centre.

The Colour of the Sphalerite from the Hosokura Mine, Miyagi Prefecture (*Part II*) (pp. 24-33)

Kenji Togari

Following the results of Part I, the hue and brilliance of the sphalerite from the Hosokura Mine have been determined according to the Ostwald colour standard. The hue of the sphalerite is correlative with the wave length of its absorption peak, but not with its iron content. As the iron content in the sphalerite increases, the brilliancy decreases and the lattice distance of (531) increases. There is a general tendency that the later the stage of crystallization, the higher the iron content and the lower the cadmium content.

Helvite from Yagisawa Mine, Nagano Prefecture

(pp. 34-41)

Toyofumi Yoshimura and Mayumi Yoshinaga

A new occurrence of helvite in the manganese ore deposit of the Yagisawa mine is reported. This mineral is found as grains or rough pyramidal crystals, often as large as 2~1 cm. across. $H=6$, $d_4^{25°}=3.21$, colour amber-yellow to siskin-green, often brownish green. $n=1.736$. X-ray powder photographs were examined. Large amount of BeO was detected spectroscopically, accompanied by other essential components, such as Fe, Mn, Si. Occurs in the siliceous manganese ore, associated with rhodonite, pyroxmangite, spessartite, fluorite and quartz. Minor associates are tephroite, alleghanyite, hübnerite, alabandite, marmatite and other sulphide minerals.

A Simple Device for Constructing Crystal Structure Models (pp. 42-48)

Yoshio Takéuchi

In the present paper, a device for drilling orientated holes in spheres which are required for the construction of crystal structure models is described, and examples of models which have been constructed by the use of the device are given. The mechanism of the device is similar with that of Buerger's machine (Rev. Sci. Inst., 6, 412, 1935) except *clamping device of spheres* and routine three steps of the procedure for drilling a hole, i.e. (1) clamping the spheres tightly, (2) drilling a hole and then (3) opening the clamp for the change of orientation, can be performed automatically through a single operation, providing less effort for drilling holes in a sphere from various directions.

Short Communications

Communications on Minerals of Japan (*Part* 14)

(pp. 49-55)

Mumeikai Group

38. *Phosphuranylite from Shiozawa, Fukushima Prefecture*

Kin-ichi Sakurai and Akira Kato

Fine platy crystals of phosphuranylite occur in the pegmatite of Shiozawa, accompanied by autunite. X-ray powder lines and refractive indices are given.

39. *Mottramite from the Munakuni Mine, Yamaguchi Prefecture*

Kin-ichi Sakurai and Akira Kato

Mottramite from the Munakuni mine forms an earthy crust of yellowish grey colour and is accompanied by chrysocolla. The results of X-ray powder method and fluorescent X-ray spectrography are given.

Reviews

The Age Determination of Minerals..... Nobuo Katayama and Toshio Kato.... 56- 81
Chlorite ..... Haruo Shirozu.... 82- 99
The Establishment of the International Mineralogical Association ..... Teiichi Ito....100-105
Proceedings 109-134

INDEX TO VOLUME 2

Reference pages to original articles of the Mineralogical Journal are distinguished by bold face figures. Those to abstracts of the Kobutsugaku Zasshi, the Journal of the Mineralogical Society of Japan, are in ordinary type.

Abukumalite from Suishoyama (Sakurai) 207
Abuta mine, cristobalite from,..351
Adati, K. and Hariya, Y. Studies of limonite ore from the Shinmen mine, Hokkaido.....339
Adularia and orthoclase from Banda, on the growth relation of (Tomisaka et al.)..... 61
Akiba, C. Common augite from Neppu, Shiribeshi province, Hokkaido 352
Akita Pref., diaspore from the Hanaoka mine.....187
——, glauconite from the Oga peninsula 140
Allanite, dielectric dispersion of (Kakitani) 60
Amphiboles, alkali, elliptic vibration of light in (Shoda)....269
Analcime from Mazé (Kiriyama and Azumi) 281
Anhydrite, cause of colouring of (Togari).....428
Aragonite, experimental condition favourable for the formation of (Harada and Goto)....141
Arima, clay from,.....140
Augite from Neppu (Akiba) ..352
Autunite from the Ningyô pass (Soma) 201
Azumi, M. with Kiriyama, R. Optical anomaly of analcime from Mazé, Niigata Pref.....281
$BaAl_2Si_2O_8$, hexagonal, structure with reference to its α-β inversion (Takéuchi).....311
Banda, Orthoclase and adularia from, ... 61
Bementite from the Ichinomata mine (Yoshimura et al.) 336
Bentonites, zeolite-bearing (Hayashi and Sudo).....196
Biotite, lithian, from the Takatori mine (Kato) 333
Bismuth mineral, Ikunolite from the Ikuno mine (Kato) 397
Boehmite in some "rôseki" deposits (Ota and Yamamoto)..206
—— in "rôseki" (Harada and Mitsuda) 206
Borate polyatomic ions, infrared absorption and structure of (Takéuchi) 245
Borax, crystal structure of (Morimoto) 1

Carnallite, rubidium and cesium in (Matsuda) 339
Cassiterite, ninelings of (Marumo) 202
Celestine from the Udô mine (Mukae) 142
Cell dimensions of some chlorites in Japan (Shirozu) 209
Chlorite from Usagiyama (Shirozu) 298
—— in the so-called propylite of

the Yugashima mine (Fujiwara) 200
Chlorites in Japan, X-ray powder patterns and cell dimensions of (Shirozu).....209
Clay from Arima (Kakitani) ..140
—— iron-stone in the Horokabetsu formation (Ikegami) 342
—— mineral, long spacing, from the Uku mine (Mitsuda) 169
—— ——, nickeliferous, from Niû Mine (Kinoshita et al.)..337
—— minerals, infrared absorption (Kakitani) 62
—— —— of weathering and sedimentary origins from the Higashiyama district (Tsuzuki) 142
Coquimbite from Kônomai Mine (Sakurai et al.) 352
Corundum, impurities of synthetic (Imai) 200
Cristobalite, artificial (Kagami) 344
—— from the Abuta mine (Urashima) 351
Crystal growth of hematite from Ayumikotan (Sunagawa) 340
—— lattices of indium tellurides and selenides (Sugaike)..... 63
—— structure models, a simple device for constructing (Takéuchi) 421
—— —— of borax (Morimoto).. 1
—— —— of vonsenite (Takéuchi) 19
Crystalline schists, special minerals in the Kamuikotan (Suzuki) 346

Deweylite from Horokanai-mura (Minato and Muraoka) 345
Diaspore found in association with zincblende and pyrite ores of the Hanaoka mine (Sudo and Hayashi).....187
Dielectric dispersion of allanite (Kakitani) 60
—— phenomena of low quartz (Kiriyama and Kawai) 344

Ebisu mine, monazite from,....224
Electrical properties of indium tellurides and selenides (Sugaike) 63
Elliptic vibration of light in heikolite (Shoda) 114
—— —— —— in some alkali amphiboles (Shoda) 269
Enstatite, chromian, from Hirosé Mine (Kitahara).....340
Equilibrium relations among some manganese minerals introduced during the epoch of thermal metamorphism (Yoshinaga) 280
Ezobanryu limestone cave, stalactite from,.....341

Feldspar, structural changes of schiller-, due to the heat treatment (II) (Tomisaka et at.) 141
Fergusonite from Takehara (Sakurai et al.) 354
Fujiwara, T. Chlorite in the so-called propylite of the Yugashima mine 200
Fujiyama, I. with Sakurai, K. et al. Coquimbite from Kônomai Mine, Hokkaido 352
—— ——. Roemerite from Kônomai Mine, Hokkaido 353
—— ——. Voltaite from Kônomai Mine, Hokkaido.....353
Fukui, T. Mineralogical study on the stone in glass 355
Fukuoka Pref., aluminian ser-

pentine and associated chlorite from Usagiyama 298
——, sepiolite from Yoshikawa-mura 279
Fukushima Pref., abukumalite from Suishoyama 207
——, β-uranophane from Tochimoto 203
——, ferri-phlogopite from Teshirogi district 345
——, maghemite from Takanokura Mine.....337
——, Mg-vermiculite from Odaka and Uzuminé.....337
——, phosphuranylite from Shiozawa 430
——, uraninite from Fusamata, Tochimoto and Shiozawa 202
Fusamata, uraninite from, ...202

Gifu Pref., monazite from the Ebisu mine.....224
——, ninelings of cassiterite from Naégi 202
Glass, stone in (Fukui) 355
Glauconite from the Oga peninsula (Honda).....140
Goto, M. On the solubility of ionic salts 59
——. Stalactite from the Ezobanryu limestone cave, Tomamura, Hokkaidò.....341
—— and Matsuda, S. On the heat of hydration of ions 201
—— with Harada, Z. On an experimental condition favourable for the formation of aragonite.....141
Gumma Pref., sericite from Ozawa-mura 151

Hanaoka mine, diaspore from,..187
Harada, Z. and Goto, M. On an experimental condition favourable for the formation of aragonite.....141
—— and Hariya, Y. On the iron distribution in rhodochrosite from the Imai-Isizaki mine, Hokkaido 279
—— and Mitsuda, T. Boehmite in "rôseki".....206
—— with Hariya, Y. Studies on manganese-wads from some localities in Hokkaido.... ...205
Hariya, Y. Some manganese dioxide minerals in Hokkaido and their geological occurrence 342
—— and Harada, Z. Studies on manganese-wads from some localities in Hokkaido.....205
—— with Adati, K. Studies of limonite ore from the Shinmei mine, Hokkaido 339
—— with Harada, Z. On the iron distribution in rhodochrosite from the Imai-Isizaki mine, Hokkaido 279
Hayashi, H. and Sudo, T. Zeolite-bearing bentonites 196
——, with Sudo, T. Diaspore found in association with zinc-blende and pyrite ores of the Hanaoka mine, Akita Pref. ..187
Heat of hydration of ions (Goto and Matsuda) 201
Heikolite, dependence of the optical absorption on the crystallographic orientation in (Shoda) 39
——, elliptic vibration of light in (Shoda).....114
Helvite from Yagisawa Mine (Yoshimura and Yoshinaga)..429
Hematite from Ayumikotan, crystal growth of (Sunagawa) ..340
Henmi, K. Natural occurrences

of zeunerite..... .134
—— and Otsuka, H. Powellite from the Kokurobé mine, Toyama Pref. 202
—— with Tomisaka, T. and Shibuya, G. On the growth relations of orthoclase and adularia from Banda, Tôji-machi, Okayama Pref. 61
Higashiyama district, clay minerals from,.....142
Hirosé Mine, chromian enstatite from, ...340
Hirowatari, F. with Yoshimura, T. and Shirozu, H. Bementite and pyroxmangite from the Ichinomata mine, Kumamoto Pref. 336
Hokkaido, common augite from Neppu.....352
——, coquimbite from Kônomai Mine 352
——, cristobalite from the Abuta mine 351
——, deweylite from Horokanai-mura 345
——, limonite ore from the Shinmei mine 339
——, manganese dioxide minerals 342
——, manganese-wads from, ..205
——, rhodochrosite from the Imai-Isizaki mine 279
——, roemerite from Kônomai Mine 353
——, sphalerite from the Shimokawa mine 348
——, stalactite from the Ezoban-ryu limestone cave 341
——, voltaite from Kônomai Mine 353
Honda, S. Glauconite from the Oga peninsula, Akita Pref. ..140
Honda, T. with Kinoshita, K. and Tanaka, N. Nickeliferous clay mineral from Niû Mine, Oita Pref. 337
Horokabetsu formation, clay iron-stone in,.....342
Horokanai-mura, deweylite from, ...345
Hosokura mine, sphalerite from, ...428
Hübnerite from the Kaso mine (Kato).....282
Hydrothermal reaction of zeolites (Kiriyama et al.) 139

Ibaragi Pref., β-uranophane from Yamanoo 208
——, lithian biotite from the Takatori mine 333
Ichinomata mine, bementite and pyroxmangite from,.....336
Iitaka, Y. The measurement of the integrated intensity by means of a single crystal X-ray diffractometer.....283
Ikegami, S. Preliminary note on the clay iron-stone in the Horokanai formation in the Ishikari coal field 342
Ikeshiro mine, a mineral resembling todorokite from,.....203
Ikunolite, a new mineral from the Ikuno mine (Kato) 397
Imai, T. Studies on the impurity of synthetic corundum ..200
—— and Kaneko, H. Studies on manganese ores (I), Determination of quartz content 59
Imai-Isizaki mine, rhodochrosite from, ...279
Imayoshi, T. with Sakurai, K. et al. Coquimbite from Kônomai Mine, Hokkaido 352
—— ——. Roemerite from Kônomai Mine, Hokkaido.....353

—— ——. Voltaite from Kônomai Mine, Hokkaido.....353
Indium tellurides and selenides, synthesis, crystal lattices and some electrical properties of (Sugaike).....63
Infrared absorption and structures of borate polyatomic ions (Takéuchi).....245
—— —— for some clay minerals (Kakitani).....62
Ionic salts, stability of (Goto)..59
Iron sulphides in calcareous nodule (Ishibashi).....343
Ishibashi, M. On iron sulphides in calcareous nodule.....343
Ishikari coal field, clay ironstone in the Horokabetsu formation.....342
Ishikawa Pref., uraninite from Nagatejima.....202
Iwaté Pref., minerals of the Noda-Tamagawa mine.....408

Kagami, T. On the artificial cristobalite.....344
Kagoshima, Pref., nacrite-bearing kaolin clay from the Kasuga mine.....103
Kakitani, S. Dielectric dispersion of allanite.....60
——. Some properties of the clay from Arima.....140
——. Studies on infrared absorption for some clay minerals..62
Kamuikotan crystalline schists, special minerals in.....346
Kaneko, K. with Imai, T. Studies on manganese ores (I), Determination of quartz content..59
Kanematsu, S. X-ray diffraction study of silicified wood.....206
Kaolin minerals in "rôseki" (Takeshi).....280
Kaso mine, hübnerite from,....282
Kasuga mine, nacrite-bearing kaolin clay from,.....103
Kato, A. β-uranophane from Yamanoo, Ibaragi Pref.....208
——, Hübnerite from the Kaso mine, Tochigi Pref.....282
——. Ikunolite, a new bismuth mineral from the Ikuno mine, Japan.....397
—— with Nagashima, O. β-uranophane from Tochimoto, Fukushima Pref.....203
—— ——, and Sakurai, K. Uraninite from Fusamata, Tochimoto and Shiozawa, Fukushima Pref.....202
—— with Ogushi, N. Szomolnokite and mirabilite from the Yanahara mine, Okayama Pref.....282
—— with Ogushi, N. et al. Voltaite from the Yanahara mine, Okayama Pref.....282
—— with Sakurai, K. Mottramite from the Munakuni mine, Yamaguchi Pref.....430
—— ——. Phosphuranylite from Shiozawa, Fukushima Pref..430
—— ——. Uraninite from Nagatejima, Ishikawa Pref.....202
—— —— and Tabata, S. Monazite and fergusonite from Takehara, Mié Pref.....354
—— —— ——. Xenotime from Takehara, Mié Pref.....353
—— —— et al. Coquimbite from Kônomai Mine, Hokkaido....352
—— —— ——. Roemerite from Kônomai Mine, Hokkaido....353
—— —— ——. Voltaite from Kônomai Mine, Hokkaido....353
—— with Watanabe, T. A new occurrence of pyrosmalite in

the Kyurazawa mine, Tochigi Pref., Japan 180
Kato, T. A study on monazite from the Ebisu mine, Gifu Pref. 224
——. Lithian biotite from the Takatori mine, Ibaragi Pref. .333
Kawai, S. with Kiriyama, R. Dielectric phenomena of low quartz 344
Kawakami, T. with Ukai, Y. and Kimura, Y. The relation between the munite content of uranium in zircon and its mineralogical characters 350
Kimura, Y. with Ukai, Y. and Kawakami, T. The relation between the munite content of uranium in zircon and its mineralogical characters 350
Kinoshita, K., Tanaka, N. and Honda, T. Nickeliferous clay mineral from Niû Mine, Oita Pref. 337
Kiriyama, R. and Azumi, M. Optical anomaly of analcime from Mazé, Niigata Pref. 281
—— and Kawai, S. Dielectric phenomena of low quartz 344
——, Koizumi, M., Yamada, K. and Kitagaki, R. Hydrothermal reaction of zeolites 139
Kitagaki, R. with Kiriyama, R. et al. Hydrothermal reaction of zeolites 139
Kitahara, J. Chromian enstatite from Hirosé Mine, Tari district, Tottori Pref. 340
Kodama, H. Mineralogical study on some pyrophyllites in Japan 236
——. Sericite from Ozawa-mura, Gumma Pref. 151
Koizumi, M. with Kiriyama, R. et al. Hydrothermal reaction of zeolites 139
Kokurobé mine, powellite from, .202
Kônomai mine, coquimbite from, ...352
——, roemerite from, ...353
——, voltaite from, ...353
Kumamoto Pref., bementite and pyroxmangite from the Ichinomata mine 336
Kumano mine, maghemite from, ...346
Kyurazawa mine, pyrosmalite from, ...180

Limonite ore from Shinmei mine (Adati and Hariya) 339
Lithium micas from the pegmatite of Minagi (Ukai et al.).. 27

Maghemite from Takanokura Mine (Takeuchi and Nambu) ..337
—— from the Kumano mine (Shibuya) 346
Magnesium-borate minerals in dolomite contact skarns (Watanabe) 351
Manganese dioxide minerals in Hokkaido (Hariya) 342
—— minerals, equilibrium relations among, of thermal metamorphism (Yoshinaga) 280
—— ores, determination of quartz content in (Imai and Kaneko) 59
Manganese-wads from some localities in Hokkaido (Hariya and Harada) 205
Manganite from the Oyé mine, Niigata Pref. (Takasu) 207
Marumo, F. On the ninelings of cassiterite from Naégi, Gifu Pref. 202
Matsuda, S. On the rubidium

and cesium in carnallite 339
—— with Goto, M. On the heat of hydration of ions.....201
Matsuoka, M. with Sudo, T. Crystallization of volcanic glass by alkali solutions 338
Mazé, analcime from,.....281
——, iron-rich saponite from, ..193
Melilite crystal in the cavity of blast-furnace slag (Minato)..422
Micas, apparent polytypism and apparent cleavage in (Takano and Takano) 347
Mié Pref., monazite and fergusonite from Takehara.....354
——, xenotime from Takehara..353
Mimetite-pyromorphite series found in Japan (Rept. 2) (Muta) 60
Minagi, lithium micas from, .. 27
Minato, H. Melilite crystal in the cavity of blast-furnace slag 422
—— and Muraoka, H. Deweylite from Horokanai-mura, Hokkaido.....345
—— with Muraoka, H. et al. Sepiolite from Yoshikawa-mura, Fukuoka Pref. 279
Minato, T. with Takimoto, K. Spectrographic studies on some ore minerals (Part 1) Examination on the working condition 348
Mirabilite from the Yanahara mine (Ogushi and Kato) 282
Mitsuda, T. Long spacing clay mineral from the Uku mine, Yamaguchi Pref., Japan.....169
—— with Harada, Z. Boehmite in "rôseki".....206
Miyagi Pref., sphalerite from the Hosokura mine 428
Miyamoto, N. Iron-rich saponite from Mazé, Niigata Pref., Japan 193
Mixed-layer minerals, the discovery of, and its contribution to clay sciences (Sudo) 205
Monazite from Takehara (Sakurai et al.).....354
—— from the Ebisu mine (Kato)224
Morimoto, N. The crystal structure of borax 1
Mottramite from the Munakuni mine (Sakurai and Kato) 430
Mukae, M. Celestine from the Udô mine, Shimané Pref. 142
Munakuni mine, mottramite from 430
Muraoka, H., Minato, H., Takano, Y. and Okamoto, Y. Sepiolite from Yoshikawa-mura, Fukuoka Pref. 279
—— with Minato, H. Deweylite from Horokanai-mura 345
Muscovites, chemical properties, optical properties and structural types of (Tomisaka) ..349
Muta, K. On the pyromorphite-mimetite series found in Japan (Rept. 2) 60

Nacrite-bearing kaolin clay from the Kasuga mine, Kagoshima Pref. (Tokunaga) 103
Naégi, ninelings of cassiterite from, ...202
Nagano Pref., helvite from Yagisawa Mine 429
Nagashima, O. and Kato, A. β-uranophane from Tochimoto, Fukushima Pref. 203
——, Sakurai, K. and Kato, A. Uraninite from Fusamata, Tochimoto and Shiozawa, Fukushima Pref. 202
Nagatejima, uraninite from,....202

Nagoya City, clay minerals from the Higashiyama district 142
Nakamura, H. with Tomisaka, T. and Shibuya, G. Structural changes of schiller-feldspar due to the heat treatment (II) 141
Nambu, M. with Takeuchi, T. Maghemite from Takanokura Mine, Fukushima Pref. 337
Neppu, common augite from, ..352
Niigata Pref., analcime from Mazé 281
——, iron-rich saponite from Mazé 193
——, manganite from the Oyé mine 207
Ningyô pass, autunite from,....201
Niû mine, nickeliferous clay mineral from 337
Noda-Tamagawa mine, minerals of,.....408

Odaka, Mg-vermiculite from, ..337
Oga peninsula, glauconite from, ...140
Ogushi, N. Pyrite from Yanahara Mine, Okayama Pref. ..207
—— and Kato, A. Szomolnokite and mirabilite from the Yanahara mine, Okayama Pref. ..282
——, Kato, A., Sakurai, K. and Sakamaki, Y. Voltaite from the Yanahara mine, Okayama Pref. 282
Oita Pref., nickeliferous clay mineral from Niû Mine.....337
Okamoto, Y. with Muraoka et al. Sepiolite from Yoshikawa-mura, Fukuoka Pref.....279
Okayama Pref., lithium micas from Minagi 27
——, orthoclase and adularia from Banda 61
——, pyrite from Yanahara Mine 207
——, szomolnokite and mirabilite from the Yanahara mine..282
——, voltaite from the Yanahara mine 282
Okayama and Tottori Prefs., autunite from the Ningyô pass..201
Omori, K. Mode of occurrence and chemical composition of Mg-vermiculite from Odaka and Uzuminé, Fukushima Pref. 337
Optical absorption, dependence of, on the crystallographic orientation in heikolite (Shoda).. 39
—— anomaly of analcime from Mazé (Kiriyama and Azumi)..281
—— properties of some muscovites and phlogopites (Tomisaka) 349
Orthoclase and adularia from Banda, on the growth relation of (Tomisaka et al.) 61
Ota, T. and Yamamoto, T. Boehmite in some "rôseki" deposits 206
Otsuka, H. with Henmi, K. Powellite from the Kokurobé mine, Toyama Pref. 202
Oyé mine, manganite from, ...207
Ozawa-mura, sericite from, ...151

Phlogopite, ferri-, from Teshirogi district (Sambonsugi) 345
——s, chemical properties, optical properties and structural types of (Tomisaka) 349
Phosphuranylite from Shiozawa (Sakurai and Kato) 430
Plagioclases, frequency distribution of the composition of, in some igneous rocks (Sueno).. 48
Polytypism, apparent, in micas

(Takano and Takano).....347
Powellite from the Kokurobé mine (Henmi and Otsuka)....202
Precession photographs, X-ray surface reflection fields on (Takéuchi) 162
Pyrite from Yanahara Mine (Ogushi).....207
Pyromorphite-mimetite series found in Japan (Muta) 60
Pyrophyllites in Japan (Kodama) 236
Pyrosmalite from the Kyurazawa mine (Watanabe and Kato) 180
Pyroxenes of the acmite-diopside system, synthetic (Yagi) 351
Pyroxmangite from the Ichinomata mine (Yoshimura et al.). 336

Quartz, low, dielectric phenomena of (Kiriyama and Kawai)..344

Rhodochrosite, iron distribution in, from the Imai-Isizaki mine (Harada and Hariya) 279
Roemerite from Kônomai Mine (Sakurai et al.) 353

Sadanaga, R. On the theory of twinned space groups.....427
Saito, T. Studies on the impurities in metallic selenium with special reference to the properties as a rectifier 338
Saito, Y. New techniques in X-ray crystallography involving the use of anomalous dispersion 204
Sakamaki, Y. with Ogushi N. et al. Voltaite from the Yanahara mine, Okayama Pref.....282
Sakurai, K. Abukumalite from Suishoyama, Fukushima Pref. .207
—— and Kato, A. Mottramite from the Munakuni mine, Yamaguchi Pref.....430
—— ——. Phosphuranylite from Shiozawa, Fukushima Pref. ..430
—— ——. Uraninite from Nagatejima, Ishikawa Pref. 202
—— ——, Fujiyama, I. and Imayoshi, T. Coquimbite from Kônomai Mine, Hokkaido 352
—— —— —— ——. Roemerite from Kônomai Mine, Hokkaido 353
—— —— —— ——. Voltaite from Kônomai Mine, Hokkaido 353
——, Tabata, S. and Kato, A. Monazite and fergusonite from Takehara, Mié Pref. 354
—— —— ——. Xenotime from Takehara, Mié Pref. 353
—— and Takasu, S. A mineral resembling todorokite found in the Ikeshiro mine, Shizuoka Pref.....203
—— with Nagashima, O. and Kato, A. Uraninite from Fusamata, Tochimoto and Shiozawa, Fukushima Pref. 202
—— with Ogushi, N. et al. Voltaite from the Yanahara mine, Okayama Pref. 282
Sambonsugi, M. Ferri-phlogopite from Teshirogi district, Fukushima Pref. 345
Saponite, iron-rich, from Mazé (Miyamoto) ... .193
Sasaki, A. Variation of unit cell parameters in wolframite series 375
Selenium, impurities in metallic (Saito) 338
Sepiolite from Yoshikawa-mura, (Muraoka et al.) 279
Sericite from Ozawa-mura, Gum-

ma Pref. (Kodama) 151
Serpentine, aluminian, from Usagiyama (Shirozu) 298
Shibuya, G. On maghemite from the Kumano mine, Yamaguchi Pref. and its oxidation by heating 346
—— with Tomisaka, T. and Henmi, K. On the growth relation of orthoclase and adularia from Banda, Tôji-machi, Okayama Pref. 61
—— —— and Nakamura, H. Structural changes of schillerfeldspar due to the heat treatment (II) 141
Shimané Pref., celestine from the Udô mine (Mukae) 142
Shimokawa mine, sphalerite from, ...348
Shinmei mine, limonite ore from,339
Shiozawa, phosphuranylite from,430
——, uraninite from, ...202
Shirozu, H. Aluminian serpentine and associated chlorite from Usagiyama, Fukuoka Pref., Japan 298
——. X-ray powder patterns and cell dimensions of some chlorites in Japan, with a note on their interference colour 209
—— with Yoshimura, T. and Hirowatari, F. Bementite and pyroxmangite from the Ichinomata mine, Kumamoto Pref. 336
Shizuoka Pref., a mineral resembling todorokite in the Ikeshiro mine 203
Shoda, T. Dependence of the optical absorption on the crystallographic orientation in heikolite 39
——. Elliptic vibration of light in some alkali amphiboles....269
——. On probable elliptic vibration of light in heikolite 114
Silicified wood, X-ray diffraction study of (Kanematsu)..... ..206
Slag, melilite crystal in the cavity of blast-furnace (Minato)..422
Soma, T. Autunite from the Ningyô pass on the boundary between Tottori and Okayama Prefs., Japan 201
Space groups, twinned (Sadanaga) 427
Spectrographic studies on some ore minerals (Takimoto and Minato) 348
Sphalerite from the Hosokura mine, colour of (Togari) 428
—— Shimokawa mine (Togari) .348
Stalactite from the Ezobanryu limestone cave (Goto).....341
Stone in glass (Fukui) 355
Structure of hexagonal $BaAl_2Si_2O_8$ (Takéuchi) 311
Structural types of some muscovites and phlogopites (Tomisaka).....349
Sudo, T. The discovery of mixed-layer minerals and its contribution to clay sciences 205
—— and Hayashi, H. Diaspore found in association with zincblende and pyrite ores of the Hanaoka mine, Akita Pref. ..187
—— and Matsuoka, M. Crystallization of volcanic glass by alkali solutions 338
—— with Hayashi, H. Zeolite-bearing bentonites 196
Sueno, T. Frequency distribution of the composition of plagioclases in some igneous rocks 48
Sugaike, S. Synthesis, crystal lattices and some electrical

properties of indium tellurides and selenides 63
Suishoyama, abukumalite from, .207
Sunagawa, I. Crystal growth of hematite from Ayumikotan, Japan 340
Sussexite-szaibelyite series, X-ray powder diffraction patterns of (Takéuchi)..... 78
Suzuki, J. On some special minerals in the Kamuikotan crystalline schists 346
Synthesis, of indium tellurides and selenides (Sugaike)..... 63
Szaibelyite-sussexite series, X-ray powder diffraction patterns of (Takéuchi)..... 78
Szomolnokite from the Yanahara mine (Ogushi and Kato) 282

Tabata, S. with Sakurai, K. and Kato, A. Monazite and fergusonite from Takehara, Mié Pref. 354
—— —— ——. Xenotime from Takehara, Mié Pref.....353
Takano, K. with Takano, Y. Apparent polytypism and apparent cleavage in micas 347
Takano, Y. A spiral Weissenberg apparatus for X-ray analysis 143
—— and Takano, K. Apparent polytypism and apparent cleavage in micas.....347
—— with Muraoka, H. et al. Sepiolite from Yoshikawa-mura, Fukuoka Pref.....279
Takanokura mine, maghemite from, ...337
Takasu, S. Manganite from the Oyé mine, Niigata Pref.....207
—— with Sakurai, K. A mineral resembling todorokite found in the Ikeshiro mine, Shizuoka Pref. 203
Takatori mine, lithian biotite from, ...333
Takehara, monazite and fergusonite from,.....354
——, xenotime from, ...353
Takeshi, H. Kaolin minerals in "rôseki" 280
Takeuchi, T. and Nambu, M. Maghemite from Takanokura mine, Fukushima Pref. 337
Takéuchi, Y. A detailed investigation of the structure of hexagonal $BaAl_2Si_2O_8$ with reference to its α-β inversion ..311
——. A simple device for constructing crystal structure models 429
——. Infrared absorption and structure of borate polyatomic ions 245
——. The absolute structure of ullmanite, NiSbS 90
——. The crystal structure of vonsenite 19
——. The interpretation of X-ray powder diffraction patterns of the szaibelyite-sussexite series 78
——. X-ray surface reflection fields on precession photographs 162
Takimoto, K. and Minato, T. Spectrographic studies on some ore minerals (Part 1) Examination of the working conditions 348
Tanaka, N. with Kinoshita, K. and Honda, T. Nickeliferous clay mineral from Niû mine, Oita Pref.....337
Tari district, chromian enstatite from Hirosé Mine.....340

Teshirogi district, ferri-phlogopite from,.....345
Tochigi Pref., pyrosmalite from the Kyurazawa mine.....180
——, hübnerite from the Kaso mine.....282
Tochimoto, β-uranophane from,..203
——, uraninite from, ...202
Todorokite, a mineral resembling, found in the Ikeshiro mine (Sakurai and Takasu)..203
Togari, K. Cause of colouring of anhydrite (Part II) 428
——. Sphalerite from the Shimokawa mine, Hokkaido 348
——. The colour of the sphalerite from the Hosokura mine, Miyagi Pref. (Part II) 428
Tokunaga, M. Nacrite-bearing kaolin clay from the Kasuga mine, Kagoshima Pref., Japan.103
Toma-mura, stalactite from the Ezobanryu limestone cave....341
Tomisaka, T. On the chemical properties, optical properties and the structural types of some muscovites and phlogopites 349
——, Henmi, K. and Shibuya, G. On the growth relations of orthoclase and adularia from Banda, Tôji-machi, Okayama Pref. 61
——, Shibuya, G. and Nakamura, H. Structural changes of schiller-feldspar due to the heat treatment (II).....141
Tottori Pref., chromian enstatite from Hirosé Mine.....340
—— and Okayama Prefs., autunite from the Ningyô pass ..201
Toyama Pref., powellite from the Kokurobé mine 202
Tsuzuki, Y. Clay minerals of weathering and sedimentary origins from the Higashiyama district, Nagoya City 142
Twinned space groups (Sadanaga) 427

Udô mine, celestine from,.....142
Ukai, Y., Kawakami, T. and Kimura, Y. The relation between the munite content of uranium in zircon and its mineralogical characters.....350
——, Nishimura, S. and Hashimoto, Y. Chemical studies of lithium micas from the pegmatite of Minagi, Okayama Pref. 27
Uku mine, long spacing clay mineral from,.....169
Ullmanite, absolute structure of (Takéuchi) 90
Unit cell parameters, variation of, in wolframite series (Sasaki) 375
Uraninite from Fusamata, Tochimoto and Shiozawa (Nagashima et al.).....202
—— from Nagatejima (Sakurai and Kato) 202
Uranophane, β-, from Tochimoto (Nagashima and Kato) 203
——, ——, from Yamanoo (Kato) 208
Urashima, Y. Cristobalite from the Abuta mine in Hokkaido..351
Usagiyama, aluminian serpentine and associated chlorite from, ...298
Uzuminé, Mg-vermiculite from,.337

Vermiculite, Mg-, from Odaka and Uzuminé (Omori).....337
Volcanic glass, crystallization of, by alkali solutions (Sudo and Matsuda) 338

Voltaite from Kônomai Mine (Sakurai et al.) 353
—— from the Yanahara mine (Ogushi et al.) 282
Vonsenite, crystal structure of (Takéuchi) 19

Watanabe, T. On the occurrence and paragenesis of magnesium-borate minerals in dolomite contact skarns 351
——. The minerals of the Noda-Tamagawa mine, Iwaté Pref., Japan. I. Notes on geology and paragenesis of minerals..408
—— and Kato, A. A new occurrence of pyrosmalite in the Kyurazawa mine, Tochigi Pref., Japan 180
Weissenberg apparatus, a spiral, for X-ray analysis (Takano)..143
Wolframite series, variation of unit cell parameters in (Sasaki) 375

Xenotime from Takehara (Sakurai et al.) 353
X-ray crystallography, new techniques in, involving the use of anomalous dispersion (Saito) 204
—— diffractometer, measurement of the integrated intensity by means of a single crystal (Iitaka) 283

Yagi, K. Synthetic pyroxenes of the acmite-diopside system ..351
Yagisawa Mine, helvite from, ..429
Yamada, K. with Kiriyama, R., et al. Hydrothermal reaction of zeolites 139
Yamaguchi Pref., long spacing clay mineral from the Uku mine 169
——, maghemite from the Kumano mine 346
——, mottramite from the Munakuni mine.....430
Yamamoto, T. with Ota, T. Boehmite in some "rôseki" deposits 206
Yamanoo, β-uranophane from,..208
Yanahara mine, pyrite from, ..207
——, szomolnokite and mirabilite from, ...282
——, voltaite from, ...282
Yoshikawa-mura, sepiolite from, ...279
Yoshimura, T. and Yoshinaga M. Helvite from Yagisawa Mine, Nagano Pref. 429
——, Shirozu, H. and Hirowatari, F. Bementite and pyroxmangite from the Ichinomata mine, Kumamoto Pref., ...336
Yoshinaga, M. A thermodynamic study of equilibrium relations among some manganese minerals introduced during the epoch of thermal metamorphism 280
—— with Yoshimura, T. Helvite from Yagisawa mine, Nagano Pref. 429
Yugashima mine, chlorite in the so-called propylite of, ...200

Zeolite-bearing bentonites (Hayashi and Sudo).....196
Zeolites, hydrothermal reaction of (Kiriyama et al.) 139
Zeunerite, natural occurrences of (Henmi) 134
Zircon, the relation between the munite content of uranium in, and its mineralogical characters (Ukai et al.) 350

Printed by "GAKUJUTSU" Printing Co., Ltd.

Mineralogical Society of Japan

OFFICERS FOR 1959–1960

President: Teiichi Ito, University of Kyoto, Kyoto.

Vice-President: Eumpei Yoshiki, Asahi Glass Co. Ltd., Tokyo.

Secretary: Hideo Minato, University of Tokyo, Tokyo.

Treasurer: Toshio Sudo, Tokyo University of Education, Tokyo.

Editor: Tokugoro Shoda, University of Tokyo, Tokyo.

Secretary for International Activities: Nobuo Katayama, University of Tokyo, Tokyo.

Councillors: Zyunpéi Harada; Hokkaido University, Sapporo. Keiichi Omori, Tsunehiko Takeuchi; Tohoku University, Sendai. Shuichi Iwao, Nobuo Katayama, Eiichi Minami, Hideo Minato, Ryoichi Sadanaga, Tokugoro Shoda, Seitaro Tsuboi, Takeo Watanabe; University of Tokyo, Tokyo. Toshio Sudo; Tokyo University of Education, Tokyo. Teiroku Sueno; Onoda Cement Co. Ltd., Tokyo. Ichiro Sunagawa; Geological Survey of Japan, Tokyo. Kin-ichi Sakurai; Tokyo. Yasuo Ukai; University of Kyoto, Kyoto. Ryoiti Kiriyama; University of Osaka, Osaka. Kitinosuke Henmi; Okayama University, Okayama. Kameki Kinoshita, Toyofumi Yoshimura; Kyushu University, Fukuoka.

PUBLICATIONS

Kôbutsugaku Zasshi, Journal of the Mineralogical Society of Japan

A journal containing articles and reviews on mineralogy and allied sciences contributed by members of the Mineralogical Society of Japan. Published every four months, in Japanese. The price of subscription is $1.00 per single copy.

Mineralogical Journal

A journal containing articles on mineralogy and allied sciences, published semi-annually in English principally. Contributions are invited from every-one. The Journal completed its second volume of six numbers in 1959. Back numbers may be obtained at $1.00 per single copy for the time being. The price of subscription to third volume is $5.00 per volume.